

Received May 4, 2019, accepted May 17, 2019, date of publication May 22, 2019, date of current version June 5, 2019.

Digital Object Identifier 10.1109/ACCESS.2019.2918256

Multi-Sensor Multi-Target Tracking Using Probability Hypothesis Density Filter

LONG LIU[✉], HONGBING JI, (Senior Member, IEEE), WENBO ZHANG, AND GUI SHENG LIAO

School of Electronic Engineering, Xidian University, Xi'an 710071, China

Corresponding author: Long Liu (longliu@xidian.edu.cn)

This work was supported in part by the National Natural Science Foundation of China under Grant 61803288 and Grant 61503293, and in part by the China Postdoctoral Science Foundation under Grant 2018M633467.

ABSTRACT Compared with the single sensor tracking system, the multi-sensor tracking system has several advantages in target tracking, such as a larger field of view and higher tracking accuracy. Different from the multi-sensor filters based on the random finite set (RFS) theory, the product multi-sensor probability hypothesis density (PM-PHD) filter with a modified cardinality coefficient performs well in estimating the number of targets. Since the PM-PHD filter employs the iterative fusion structure, its state estimation is sensitive to the sensor parameters. Furthermore, to improve the cardinality estimation, the PM-PHD filter may estimate some false targets when miss-detection occurs. Addressing the above problems, this paper changes the fusion structure of the PM-PHD filter and presents a novel version of the PM-PHD filter. The main idea of the proposed algorithm is the combinations of measurement subsets and other factors. Both the cardinality estimation and the state estimation are obtained by fusing the target numbers and normalized PHDs of these combinations. Compared with other multi-sensor PHD filters, the proposed algorithm can handle the problems of miss-detection and false alarm effectively. Moreover, the simulation results and the theoretical analysis indicate that the new PM-PHD filter can deal with a harsh tracking environment.

INDEX TERMS Multi-sensor fusion, multi-target tracking, random finite set, probability hypothesis density.

I. INTRODUCTION

The multi-target tracking (MTT) algorithms have been used to deal with the measurement uncertainties and estimate the location, velocity, acceleration, number and trajectory of targets. The traditional MTT algorithms are mainly based on data association, such as global nearest neighbor (GNN) [1], [2], joint probabilistic data association (JPDA) [3], [4], multiple hypothesis tracking (MHT) [5], [6] and their variances [7], [8]. In general, above MTT algorithms can track the targets effectively. However, in the tracking environments with high target density and clutter density, the large computational complexity caused by data association has become the biggest obstacle to such algorithms. In this regard, Mahler combined the random finite set (RFS) [9], [10] theory with the MTT algorithms, and proposed several methods to estimate the characteristics of targets without data association. At present, the most commonly used RFS filters are probability hypothesis density (PHD)

filter [11], [12], cardinality probability hypothesis density (CPHD) filter [13] and cardinality balanced Member (CBMeMber) filter [14], [15]. The PHD filter is an approximate multi-target Bayesian filter. It is difficult to get the analytical solution of the PHD filter for the reason that the updating formulas of the PHD filter contain multiple integrals. To implement the PHD filter, Mahler and B.N. Vo proposed sequential Monte Carlo PHD (SMC-PHD) filter [16], [17] and Gaussian mixture PHD (GM-PHD) filter [18], [19] under nonlinear and linear conditions, respectively. With the increase of false alarms and miss detection, the cardinality estimation of the PHD filter becomes unstable. Therefore, Mahler proposed the CPHD filter which could update multi-target posteriori density and posterior cardinality distribution simultaneously. Although the CPHD filter performs better than the PHD filter in estimating the number of targets, it has a high computational complexity and delayed cardinality estimation. The MeMber filter [20], [21], which is originally proposed by Mahler, has the advantages of easy implementation and low computational cost. But it is only applicable to the tracking environment with high

The associate editor coordinating the review of this manuscript and approving it for publication was Jiansong Liu.

probability of detection and low clutter density. Furthermore, B.N. Vo indicated that the number of targets was overestimated by the MeMber filter and proposed the commonly used CBMeMber filter. Although the MTT algorithms based on RFS can avoid data association, it is difficult to get the complete track of targets. Thus, the track maintenance issues are gradually noticed. In [22]–[24], B.T. Vo and B.N. Vo combined the label space with the state space, and introduced the Labeled RFS and the Labeled Multi-Bernoulli RFS. Additionally, the Labeled MeMber (LMB) [25] and the Generalized Labeled MeMber (GLMB) [26] were proposed to estimate the state and track of targets simultaneously.

The above mentioned MTT algorithms are only applicable to single sensor. The single sensor tracking system is unstable and vulnerable to the tracking environment. Therefore, the multi-sensor solutions [27] attract the attention of researchers. The multi-sensor filters based on RFS are mainly applied to centralized fusion system [28]–[33]. In [28], a multi-sensor PHD filter based on measurement clustering is proposed to handle the lack of statistical knowledge of the sensors. In [29], a two-sensor PHD filter is proposed by Mahler, named General PHD filter. However, Mahler only gave the theoretical proof and updating formulas of the General PHD filter, and he did not implement the filter. In [30], Nannuru derived the general form of the General PHD filter and proposed the General CPHD filter, and he also gave the Gaussian mixture implementation of these two filters. The General PHD and CPHD filters need to partition the measurements received by all sensors and traverse all possible measurement partitions. As the numbers of sensors and measurements increase, the computational burden of the filters increases rapidly. It affects the application of such filters seriously. In [11], besides the PHD filter, Mahler also proposed an approximate multi-sensor PHD filter, named the iterated-corrector PHD (IC-PHD) filter. To avoid the data association in multi-sensor fusion, multiple single-sensor Bayesian filters are used in the IC-PHD filter to replace the multi-sensor multi-target estimation. Although the IC-PHD filter performs well in most cases, it still has some drawbacks. Comparing the tracking results under different sensor parameters, the performance of the IC-PHD filter is affected by the sensor order and probability of detection [31]. Addressing these problems, Mahler added a coefficient to the update formula of the IC-PHD filter and proposed the product multi-sensor PHD (PM-PHD) filter [32]. Although the coefficient can improve the cardinality estimation effectively, it is very difficult to be computed. In this regard, we presented an approximate solution for the coefficient and the Gaussian implementation for the PM-PHD filter [33]. Additionally, to deal with the problem that the coefficient had a negative impact on state estimation, a modified method was proposed by using the relationships between the Gaussian components, named the cardinality modified PM-PHD (CM-PM-PHD) filter. But limited by the assumptions of linear Gaussian mixture model (GMM), the CM-PM-PHD filter could not achieve good performance in the harsh tracking environment.

This paper studies on the fusion structure of the PM-PHD filter, and a heuristic multi-sensor fusion method is presented. Measurements received by sensors and other factors are divided into several combinations. The cardinality estimation and the state estimation can be obtained by fusing the number of targets and the normalized PHD of the combinations, respectively. Compared with other multi-sensor PHD filters, the proposed algorithm is insensitive to the sensor parameters and not limited to the assumptions of linear GMM. The benefits of the proposed PM-PHD filter are verified by the simulations and theoretical analysis.

The rest of this paper is organized as follows. The RFS theory and the PHD filter are described briefly in Section II. The PM-PHD filter and the problem of state estimation are introduced in Section III. The heuristic multi-sensor fusion method based on the combination of factors is presented in Section IV. Simulation results and theoretical analysis are performed in Section V. Finally, Section VI gives the conclusions.

II. BACKGROUND

The MTT algorithms are mainly used to deal with the uncertainty of the target and measurement. The former refers to the change in the number of targets caused by target birth, spawn, miss-detection and death. The latter means that the source of the measurement cannot be determined. In other words, it is unable to determine that a measurement is generated by the target or clutter. Traditional MTT algorithms based on data association have a heavy computational burden. However, algorithms based on the RFS theory can weaken data association, and they can quickly and accurately estimate the state and number of targets. In this section, a brief description of RFS and the PHD filter is given.

In the multi-target motion model, the state set and the observation set at time k are represented by $\mathbf{X}_k = \{\mathbf{x}_1, \dots, \mathbf{x}_{N_k}\}$ and $\mathbf{Z}_k = \{\mathbf{z}_1, \dots, \mathbf{z}_{M_k}\}$, respectively. Here, N_k and M_k denote the numbers of targets and measurements at time k .

Given a state RFS \mathbf{X}_{k-1} at time $k-1$, the state RFS \mathbf{X}_k at time k can be expressed by

$$\mathbf{X}_k = \left(\bigcup_{\xi \in \mathbf{X}_{k-1}} \mathbf{S}_{k|k-1}(\xi) \right) \cup \left(\bigcup_{\xi \in \mathbf{X}_{k-1}} \mathbf{B}_{k|k-1}(\xi) \right) \cup \mathbf{\Gamma}_k \quad (1)$$

Here, $\mathbf{S}_{k|k-1}(\xi)$ represents the RFS of targets which still survive at time k from $\xi \in \mathbf{X}_{k-1}$. $\mathbf{B}_{k|k-1}(\xi)$ represents the RFS of targets spawned by $\xi \in \mathbf{X}_{k-1}$. $\mathbf{\Gamma}_k$ represents the RFS of new targets which appear instantly at time k .

Given a state RFS \mathbf{X}_k at time k , the observation RFS \mathbf{Z}_k can be expressed by

$$\mathbf{Z}_k = \mathbf{K}_k \cup \left(\bigcup_{\xi \in \mathbf{X}_k} \mathbf{\Theta}_k(\xi) \right) \quad (2)$$

Here, \mathbf{K}_k represents the observation set of clutter, and $\mathbf{\Theta}_k(\xi)$ represents the observation set generated by the state ξ .

Let $D_{k|k-1}(\mathbf{x})$ and $D_k(\mathbf{x})$ denote the PHDs of the predicted density $p_{k|k-1}(\mathbf{x})$ and the posterior density $p_k(\mathbf{x})$ at time k , respectively. Then the posterior intensity can be derived by the PHD recursion,

$$\begin{aligned} D_{k|k-1}(\mathbf{x}) &= \int p_{S,k}(\boldsymbol{\xi}) f_{k|k-1}(\mathbf{x}|\boldsymbol{\xi}) D_{k-1}(\boldsymbol{\xi}) d\boldsymbol{\xi} \\ &+ \int b_{k|k-1}(\mathbf{x}|\boldsymbol{\xi}) D_{k-1}(\boldsymbol{\xi}) d\boldsymbol{\xi} + \gamma_k(\mathbf{x}) \end{aligned} \quad (3)$$

$$\begin{aligned} D_{k|k}(\mathbf{x}) &= [1 - P_{D,k}(\mathbf{x})] D_{k|k-1}(\mathbf{x}) \\ &+ \sum_{\mathbf{z} \in \mathbf{z}_k} \frac{P_{D,k}(\mathbf{x}) g_k(\mathbf{z}|\mathbf{x}) D_{k|k-1}(\mathbf{x})}{\kappa_k(\mathbf{z}) + \int P_{D,k}(\boldsymbol{\xi}) g_k(\mathbf{z}|\boldsymbol{\xi}) D_{k|k-1}(\boldsymbol{\xi}) d\boldsymbol{\xi}} \end{aligned} \quad (4)$$

Here, $\gamma_k(\cdot)$ denotes the PHD of the birth RFS $\mathbf{\Gamma}_k$ at time k , $b_{k|k-1}(\cdot|\boldsymbol{\xi})$ denotes the PHD of the spawned RFS $\mathbf{B}_{k|k-1}(\boldsymbol{\xi})$ at time k , and $\kappa_k(\cdot)$ denotes the intensity of the clutter RFS \mathbf{K}_k . $p_{S,k}(\cdot)$ and $P_{D,k}(\cdot)$ are the probabilities of survival and detection, respectively. $f_{k|k-1}(\cdot|\boldsymbol{\xi})$ and $g_k(\cdot|\cdot)$ are the state transition function and the observation likelihood function, respectively.

III. THE PRODUCT MULTI-SENSOR PHD FILTER

A. BASIC THEORY

Assume that there is a homogeneous sensor network with s sensors. The field of view (FoV) of all sensors is completely overlapping. The sensor network has been calibrated in time and space. Measurements received by the sensors in their respective coordinate systems have been converted to the same time and spatial reference system. Suppose that

$D_{k|k-1}(\mathbf{x})$ is the predicted PHD, and the measurement set of the i^{th} sensor is denoted by $\mathbf{Z}_k^i = \{\mathbf{z}_1, \dots, \mathbf{z}_m\}$, $i = 1, \dots, s$, where m is the number of measurements.

The IC-PHD filter can be represented as

$$D_{k|k}^i(\mathbf{x}) = L_{\mathbf{z}_k^i}^1(\mathbf{x}) \cdot D_{k|k}^{i-1}(\mathbf{x}) \quad i = 1, 2, \dots, s \quad (5)$$

$$D_{k|k}(\mathbf{x}) \approx D_{k|k}^s(\mathbf{x}), D_{k|k}^0(\mathbf{x}) = D_{k|k-1}(\mathbf{x}) \quad (6)$$

Here, $L_{\mathbf{z}_k^i}^i(\mathbf{x})$ is the pseudo-likelihood of the i^{th} sensor, and

$$L_{\mathbf{z}_k^i}^i(\mathbf{x}) = 1 - P_{D,k}^i(\mathbf{x}) + \sum_{\mathbf{z} \in \mathbf{z}_k^i} \frac{P_{D,k}^i(\mathbf{x}) g_k(\mathbf{z}|\mathbf{x})}{\kappa_k^i(\mathbf{z}) + D_{k|k-1}(\mathbf{x}) [P_{D,k}^i g_{\mathbf{z}}]} \quad (7)$$

Combining (5) and (6), the update formula of the IC-PHD filter can be rewritten as

$$D_{k|k}(\mathbf{x}) = L_{\mathbf{z}_k^1}^1(\mathbf{x}) \cdots L_{\mathbf{z}_k^s}^s(\mathbf{x}) \cdot D_{k|k-1}(\mathbf{x}) \quad (8)$$

Furthermore, the updated formulas of the PM-PHD filter can be described as

$$\begin{aligned} D_{k|k}(\mathbf{x}) &= \phi \cdot \frac{L_{\mathbf{z}_k^1}^1(\mathbf{x}) \cdots L_{\mathbf{z}_k^s}^s(\mathbf{x})}{v_{k|k}^1 \cdots v_{k|k}^s} \cdot D_{k|k-1}(\mathbf{x}) \end{aligned} \quad (9)$$

$$\phi = \frac{\sum_{n \geq 0} \ell_{\mathbf{z}_k^1}^1(n+1) \cdots \ell_{\mathbf{z}_k^s}^s(n+1) \cdot \frac{\left(\sum_{k|k-1}^{1,\dots,s} \eta \right)^n}{n!}}{\sum_{n \geq 0} \ell_{\mathbf{z}_k^1}^1(n) \cdots \ell_{\mathbf{z}_k^s}^s(n) \cdot \frac{\left(\sum_{k|k-1}^{1,\dots,s} \eta \right)^n}{n!}} \quad (10)$$

$$\begin{aligned} \ell_{\mathbf{z}_k^i}^i(n) &= \sum_{l_n^i=0}^{\hat{l}_n^i} \frac{l_n^i! \cdot C_n^{l_n^i} \cdot D_{k|k-1}^{1,\dots,s} \left[1 - P_{D,k}^i \right]^{n-l_n^i} \hat{\sigma}_{l_n^i}^i(\mathbf{z}_k^i)}{\left(\sum_{k|k-1}^{1,\dots,s} \eta \right)^n} \end{aligned} \quad (11)$$

$$\begin{aligned} \hat{\sigma}_{l_n^i}^i(\mathbf{z}_k^i) &= \sigma_{m,l_n^i}^i \left(\frac{D_{k|k-1}^{1,\dots,s} \left[P_{D,k}^i g_{\mathbf{z}_k^i} \right]}{\kappa_k^i(\mathbf{z}_k^i)}, \dots, \frac{D_{k|k-1}^{1,\dots,s} \left[P_{D,k}^i g_{\mathbf{z}_k^i} \right]}{\kappa_k^i(\mathbf{z}_k^i)} \right) \end{aligned} \quad (12)$$

$$C_n^{l_n^i} \stackrel{\text{def.}}{=} \frac{n!}{l_n^i! \cdot (n-l_n^i)!} \quad (13)$$

$$\eta = \frac{\sum_{k|k-1}^{1,\dots,s} \left[L_{\mathbf{z}_k^1}^1 \cdots L_{\mathbf{z}_k^s}^s \right]}{v_{k|k}^1 \cdots v_{k|k}^s} \quad (14)$$

$$v_{k|k}^i = \sum_{k|k-1}^{1,\dots,s} \left[L_{\mathbf{z}_k^i}^i \right] \quad (15)$$

$$\hat{l}_n^i = \min(n, m) \quad (16)$$

Here, n is the possible number of targets, l_n^i , $i = 1, \dots, s$ is the possible number of detected targets of the i^{th} sensor, $\sigma_{m,l_n^i}^i[\cdot]$ is the elementary symmetric function [13]. Moreover, for any function $h(x)$, we have

$$D_{k|k-1}[h] = \int h(\boldsymbol{\xi}) \cdot D_{k|k-1}(\boldsymbol{\xi}) d\boldsymbol{\xi} \quad (17)$$

and

$$v_{k|k-1}[h] = \int h(\boldsymbol{\xi}) \cdot v_{k|k-1}(\boldsymbol{\xi}) d\boldsymbol{\xi} \quad (18)$$

$$v_{k|k-1}(\mathbf{x}) = \frac{D_{k|k-1}(\mathbf{x})}{\sum_{k|k-1}^{1,\dots,s}} \quad (19)$$

$$\sum_{k|k-1}^{1,\dots,s} = \int \sum_{k|k-1}^{1,\dots,s}(\boldsymbol{\xi}) d\boldsymbol{\xi} \quad (20)$$

In the above equations, the superscript i denotes the sensor index, and a parameter with the superscript $1, \dots, s$ indicates that the parameter is determined by all sensors.

B. THE PROBLEM OF STATE ESTIMATION

Comparing the update formulas of the IC-PHD filter and the PM-PHD filter, it can be found that the biggest difference

between the two filters is the coefficient $\phi / (v_{k|k}^1 \cdots v_{k|k}^s)$. Although the coefficient can improve the cardinality estimation, it has uncertain effects on the state estimation. Because the coefficient is a scalar and only changes the amplitude of the updated PHD. For example, there are four targets in the surveillance region, ‘Target 3’ and ‘Target 4’ are undetected by the s^{th} sensor. This situation is described in Fig. 1.

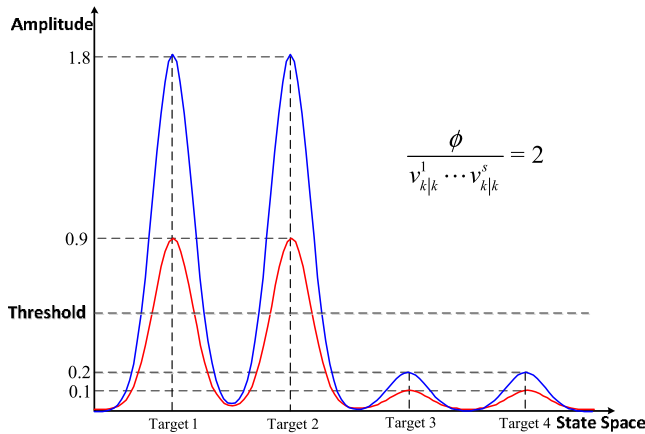


FIGURE 1. Updated PHD for four targets.

In Fig. 1, the updated PHD without $\phi / (v_{k|k}^1 \cdots v_{k|k}^s)$ is denoted by red line, and the updated PHD of the PM-PHD filter is denoted by blue line. Suppose that the uncorrected weights of ‘Target 1’ and ‘Target 2’ are approximate 0.9, the uncorrected weights of ‘Target 3’ and ‘Target 4’ is approximately 0.1. Hence, the estimated number of targets is 2. The ‘Target 3’ and ‘Target 4’ cannot be estimated, because their weights are small than the threshold [19]. To maintain the cardinality estimation, $\phi / (v_{k|k}^1 \cdots v_{k|k}^s)$ may be equal to 2. Then, the corrected number of targets is 4. However, ‘Target 3’ and ‘Target 4’ are still not estimated, because their weights are 0.2. Furthermore, in order to be consistent with the estimated number of targets, the PM-PHD filter estimates two false targets from ‘Target 1’ and ‘Target 2’.

IV. THE TWO STEPS PM-PHD FILTER

A. CARDINALITY ESTIMATION

Then, (10) can be rewritten as

$$\phi = \frac{\sum_{n \geq 0} n \cdot \mathcal{L}(n)}{\sum_{n \geq 0} \mathcal{L}(n)} \cdot \frac{1}{N_{k|k-1} \cdot \eta} \quad (21)$$

$$\mathcal{L}(n) = \prod_{i=1}^s \ell_{z_k^i}^i(n) \cdot \frac{\left(N_{k|k-1} \cdot \eta \right)^n}{n!} \quad (22)$$

Based on (14), (18), (19), and (21), (9) can be rewritten as

$$\begin{aligned} D_{k|k}^{1, \dots, s}(\mathbf{x}) &= \frac{\sum_{n \geq 0} n \cdot \mathcal{L}(n)}{\sum_{n \geq 0} \mathcal{L}(n)} \cdot \frac{L_{z_k}^1(\mathbf{x}) \cdots L_{z_k}^s(\mathbf{x}) \cdot D_{k|k-1}^{1, \dots, s}(\mathbf{x})}{\int L_{z_k}^1(\xi) \cdots L_{z_k}^s(\xi) \cdot D_{k|k-1}^{1, \dots, s}(\xi) d\xi} \\ &= \left(\sum_{n \geq 0} w_n^{1, \dots, s} \cdot N_n^{1, \dots, s} \right) \cdot v_{k|k}^{1, \dots, s}(\mathbf{x}) \end{aligned} \quad (23)$$

Here,

$$N_n^{1, \dots, s} = n \quad (24)$$

$$w_n^{1, \dots, s} = \frac{\mathcal{L}(n)}{\sum_{n \geq 0} \mathcal{L}(n)} \quad (25)$$

$$v^{1, \dots, s}(\mathbf{x}) = \frac{D^{1, \dots, s}(\mathbf{x})}{\int D^{1, \dots, s}(\xi) d\xi} \quad (26)$$

$$D^{1, \dots, s}(\mathbf{x}) \stackrel{\text{def.}}{=} L_{z_k}^1(\mathbf{x}) \cdots L_{z_k}^s(\mathbf{x}) \cdot D_{k|k-1}^{1, \dots, s}(\mathbf{x}) \quad (27)$$

Integrating both sides of (23), we have

$$N_{k|k}^{1, \dots, s} = \sum_{n \geq 0} w_n^{1, \dots, s} \cdot N_n^{1, \dots, s} \quad (28)$$

Here, $N_n^{1, \dots, s}$ denotes the number of targets, and $w_n^{1, \dots, s}$ is the weight that $N_n^{1, \dots, s}$ is correct. It can be seen that the cardinality estimation is computed by (28) directly, and the state estimation is determined by $v^{1, \dots, s}(\mathbf{x})$. From (8) and (27), it can be observed that $v^{1, \dots, s}(\mathbf{x})$ is obtained by the IC-PHD filter, and thus the state estimation of the PM-PHD filter is still sensitive to the probability of detection and sensor order. To address the problem of state estimation, a new calculation method for $v^{1, \dots, s}(\mathbf{x})$ is described below.

B. THE PROBLEM OF STATE ESTIMATION

1) The combination of factors

To facilitate description, (11) can be rewritten as

$$\ell_{z_k^i}^i(n) = \sum_{l_n^i=0}^{l_n^i} \varphi_n^i(l_n^i) \mathcal{S}_{n, l_n^i}^i(\mathbf{z}_k^i) \quad (29)$$

$$\varphi_n^i(l_n^i) = \frac{l_n^i! \cdot C_n^{l_n^i}}{\left(N_{k|k-1} \right)^n} \quad (30)$$

$$\mathcal{S}_{n, l_n^i}^i(\mathbf{z}_k^i) = \sum_{W_{r, l_n^i}^i \in \mathcal{D}_{l_n^i}^i} \prod_{z \in W_{r, l_n^i}^i} D[L_z^i] \quad (31)$$

$$L_z^i(\mathbf{x}) = \begin{cases} (1 - P_{D,k}^i(\mathbf{x})) & \mathbf{z} = \mathbf{z}_0^i \\ \frac{P_{D,k}^i(\mathbf{x}) g_k(\mathbf{z}|\mathbf{x})}{\kappa_k^i(\mathbf{z})} & \mathbf{z} \neq \mathbf{z}_0^i \end{cases} \quad (32)$$

Here, \mathbf{z}_0^i denotes the measurement of miss-detection of the i^{th} sensor. The measurement division $\mathcal{D}_{r,l_n^i}^i \Xi \mathbf{Z}_k^i$ denotes a process which consists of two parts: 1) dividing \mathbf{Z}_k^i into different measurement subsets $\hat{W}_{r,l_n^i}^i, r = 1, \dots, C_{i,m}^{l_n^i}$; 2) combining each $\hat{W}_{r,l_n^i}^i$ with $\hat{W}_{l_n^i}^i$. The combined set is denoted by $W_{r,l_n^i}^i$, and $W_{r,l_n^i}^i = \hat{W}_{r,l_n^i}^i \cup \hat{W}_{l_n^i}^i$. Here, $\hat{W}_{l_n^i}^i$ is a set that consists of \mathbf{z}_0^i , and $\hat{W}_{l_n^i}^i = \{\mathbf{z}_0^i, \dots, \mathbf{z}_0^i\}$, the number of measurements in $\hat{W}_{l_n^i}^i$ is $|\hat{W}_{l_n^i}^i| = \hat{l}_n^i - l_n^i$. Thus, $\mathcal{D}_{r,l_n^i}^i \Xi \mathbf{Z}_k^i = \{W_{1,l_n^i}^i, \dots, W_{C_{i,m}^{l_n^i}, l_n^i}^i\}$.

For example, suppose that $\mathbf{Z}_k^i = \{\mathbf{z}_1^i, \mathbf{z}_2^i, \mathbf{z}_3^i\}, m = 3, \hat{l}_n^i = 3$ and $l_n^i = 0, 1, 2, 3$. Then, $\hat{W}_{r,l_n^i}^i, r = 1, \dots, C_{i,m}^{l_n^i}$ are given by

$$\begin{aligned} \hat{W}_{1,0}^i &= \{\emptyset\} \\ \hat{W}_{1,1}^i &= \{\mathbf{z}_1^i\}, \hat{W}_{2,1}^i = \{\mathbf{z}_2^i\}, \hat{W}_{3,1}^i = \{\mathbf{z}_3^i\} \\ \hat{W}_{1,2}^i &= \{\mathbf{z}_1^i, \mathbf{z}_2^i\}, \hat{W}_{2,2}^i = \{\mathbf{z}_1^i, \mathbf{z}_3^i\}, \hat{W}_{3,2}^i = \{\mathbf{z}_2^i, \mathbf{z}_3^i\} \\ \hat{W}_{1,3}^i &= \{\mathbf{z}_1^i, \mathbf{z}_2^i, \mathbf{z}_3^i\} \end{aligned} \quad (33)$$

and $\mathcal{D}_0^i \Xi \mathbf{Z}_k^i, \dots, \mathcal{D}_3^i \Xi \mathbf{Z}_k^i$ are given by

$$\begin{aligned} \mathcal{D}_0^i \Xi \mathbf{Z}_k^i &= \{\{\mathbf{z}_0^i, \mathbf{z}_0^i, \mathbf{z}_0^i\} \cup \{\emptyset\}\} \\ \mathcal{D}_1^i \Xi \mathbf{Z}_k^i &= \{\{\mathbf{z}_1^i\} \cup \{\mathbf{z}_0^i, \mathbf{z}_0^i\}, \{\mathbf{z}_2^i\} \cup \{\mathbf{z}_0^i, \mathbf{z}_0^i\}, \{\mathbf{z}_3^i\} \cup \{\mathbf{z}_0^i, \mathbf{z}_0^i\}\} \\ \mathcal{D}_2^i \Xi \mathbf{Z}_k^i &= \{\{\mathbf{z}_1^i, \mathbf{z}_2^i\} \cup \{\mathbf{z}_0^i\}, \{\mathbf{z}_1^i, \mathbf{z}_3^i\} \cup \{\mathbf{z}_0^i\}, \{\mathbf{z}_2^i, \mathbf{z}_3^i\} \cup \{\mathbf{z}_0^i\}\} \\ \mathcal{D}_3^i \Xi \mathbf{Z}_k^i &= \{\{\emptyset\} \cup \{\mathbf{z}_1^i, \mathbf{z}_2^i, \mathbf{z}_3^i\}\} \end{aligned} \quad (34)$$

From (22), (28), (29), and (31), it can be seen that $N_{k|k}^{1,\dots,s}$ is the result of multiple fusion process. Expanding the symbols \sum and \prod in (22), (28), (29), and (31), $N_{k|k}^{1,\dots,s}$ can be rewritten in the following form

$$\begin{aligned} N_{k|k}^{1,\dots,s} &= w_{c_1} \cdot N_{c_1} + w_{c_2} \cdot N_{c_2} + \dots + w_{c_{\mathcal{T}}} \cdot N_{c_{\mathcal{T}}} \\ &= \sum_{t=1}^{\mathcal{T}} w_{c_t} \cdot N_{c_t} \\ w_{c_t} &= \frac{\binom{1,\dots,s}{N_{k|k-1} \cdot \eta}^n}{n! \cdot \sum_{n \geq 0} \mathcal{L}(n)} \cdot \prod_{i=1}^s \varphi_n^i(l_n^i) \cdot \sum_{\mathbf{z} \in W_{r,l_n^i}^i} D[L_{\mathbf{z}}^i] \end{aligned} \quad (35)$$

Here, c_t denotes the t^{th} possible combination that consists of different factors, and it is expressed by

$$c_t \stackrel{\text{def.}}{=} n, l_n^1, \dots, l_n^s, W_{r,l_n^1}^1, \dots, W_{r,l_n^s}^s \quad (37)$$

To further explain the idea of combinations, an example is given below. Suppose that there are two targets and two sensors. The measurement sets of two sensors are $\mathbf{z}_k^1 = \{\mathbf{z}_1^1, \mathbf{z}_2^1, \mathbf{z}_3^1\}$ and $\mathbf{z}_k^2 = \{\mathbf{z}_1^2, \mathbf{z}_2^2\}$, respectively. Here, \mathbf{z}_1^1 and \mathbf{z}_1^2 are the measurements of ‘Target 1’, \mathbf{z}_2^1 is the measurement

TABLE 1. The possible combinations.

n	l_n^1	l_n^2	$W_{r,l_n^1}^1 \in \mathcal{D}_{r,l_n^1}^1 \Xi \mathbf{Z}_k^1$	$W_{r,l_n^2}^2 \in \mathcal{D}_{r,l_n^2}^2 \Xi \mathbf{Z}_k^2$
c_1	0	0	\emptyset	\emptyset
c_2	1	0	$\{\mathbf{z}_0^1\}$	$\{\mathbf{z}_0^2\}$
c_3	1	0	$\{\mathbf{z}_0^1\}$	$\{\mathbf{z}_0^2, \mathbf{z}_1^2\}$
\vdots	\vdots	\vdots	\vdots	\vdots
c_t	2	2	$\{\mathbf{z}_1^1, \mathbf{z}_2^1\}$	$\{\mathbf{z}_0^2, \mathbf{z}_1^2\}$
\vdots	\vdots	\vdots	\vdots	\vdots
c	∞	3	$\{\mathbf{z}_0^1, \dots, \mathbf{z}_0^1, \mathbf{z}_1^1, \mathbf{z}_2^1, \mathbf{z}_3^1\}$	$\{\mathbf{z}_0^2, \dots, \mathbf{z}_0^2, \mathbf{z}_1^2, \mathbf{z}_2^2\}$

of ‘Target 2’, \mathbf{z}_3^1 and \mathbf{z}_2^2 are the measurements of clutter. The measurements of miss-detection of two sensors are denoted by \mathbf{z}_0^1 and \mathbf{z}_0^2 , respectively. The combinations $c_1, c_2, \dots, c_{\mathcal{T}}$ are given in Table 1. Here, \mathcal{T} is the number of combinations. In all combinations $c_1, c_2, \dots, c_{\mathcal{T}}$, there is only one correct combination. Here, w_{c_t} is the weight that c_t is the correct combination. Moreover, N_{c_t} is the number of targets corresponding to c_t .

2) The solution of state estimation

Suppose that $c_t, t = 1, \dots, \mathcal{T}$ has a corresponding normalized PHD $v_{c_t}(\mathbf{x}), t = 1, \dots, \mathcal{T}$. Then, $v^{1,\dots,s}(\mathbf{x})$ in (23) can be obtained by

$$v^{1,\dots,s}_{k|k}(\mathbf{x}) = w_{c_1} \cdot v_{c_1}(\mathbf{x}) + w_{c_2} v_{c_2}(\mathbf{x}) + \dots + w_{c_{\mathcal{T}}} \cdot v_{c_{\mathcal{T}}}(\mathbf{x}) \quad (38)$$

In the factors $n, l_n^1, \dots, l_n^s, W_{r,l_n^1}^1, \dots, W_{r,l_n^s}^s$, only $W_{r,l_n^1}^1, \dots, W_{r,l_n^s}^s$ affect $v_{c_t}(\mathbf{x}), t = 1, \dots, \mathcal{T}$. Assumed $v_{W_{r,l_n^1}^1}^1(\mathbf{x}), \dots, v_{W_{r,l_n^s}^s}^s(\mathbf{x})$ are the normalized PHDs of $W_{r,l_n^1}^1, \dots, W_{r,l_n^s}^s$, respectively. $v_{c_t}(\mathbf{x}), t = 1, \dots, \mathcal{T}$ can be obtained by fusing $v_{W_{r,l_n^1}^1}^1(\mathbf{x}), \dots, v_{W_{r,l_n^s}^s}^s(\mathbf{x})$, and we have

$$v_{c_t}(\mathbf{x}) = \sum_{i=1}^s w_n^i \cdot v_{W_{r,l_n^i}^i}^i(\mathbf{x}) \quad (39)$$

Here, w_n^i denotes the weight of the i^{th} sensor, and it indicates the accuracy of measurements received by the i^{th} sensor. However, it is difficult to determine the accuracy of measurements in $W_{r,l_n^1}^1, \dots, W_{r,l_n^s}^s$ and the accuracy of $v_{W_{r,l_n^1}^1}^1(\mathbf{x}), \dots, v_{W_{r,l_n^s}^s}^s(\mathbf{x})$. Therefore, $v_{c_1}(\mathbf{x}), t = 1, \dots, \mathcal{T}$ is computed as the average of $v_{W_{r,l_n^i}^i}^i(\mathbf{x})$, and w_n^i is set to be $\frac{1}{s}$. Then, we have (40)-(42).

$$v_{c_t}(\mathbf{x}) = \sum_{i=1}^s \frac{1}{s} \cdot v_{W_{r,l_n^i}^i}^i(\mathbf{x}) \quad (40)$$

$$v_{W_{r,l_n^i}^i}^i(\mathbf{x}) = \frac{\sum_{\mathbf{z} \in W_{r,l_n^i}^i} v_{\mathbf{z}}^i(\mathbf{x})}{\int \sum_{\mathbf{z} \in W_{r,l_n^i}^i} v_{\mathbf{z}}^i(\xi) d\xi} \quad (41)$$

$$v_{\mathbf{z}}^i(\mathbf{x}) = \frac{L_{\mathbf{z}}^i(\mathbf{x}) \cdot D_{k|k-1}(\mathbf{x})}{\int L_{\mathbf{z}}^i(\xi) \cdot D_{k|k-1}(\xi) d\xi} \quad (42)$$

Here, $v_{\mathbf{z}}^i(\mathbf{x})$ is the normalized PHD of measurement $\mathbf{z} \in W_{r,l_n^i}^i$.

Since the factor n ($n \geq 0$) is infinite, the number of combinations \mathcal{T} is infinite, too. Therefore, $v_{k|k}^{1,\dots,s}(\mathbf{x})$ cannot be obtained by (38) directly. To calculate $v_{k|k}^{1,\dots,s}(\mathbf{x})$, the terms in (38) are merged, and we have

$$v_{k|k}^{1,\dots,s}(\mathbf{x}) = \sum_{n \geq 0} w_n^{1,\dots,s} \cdot v_n^{1,\dots,s}(\mathbf{x}) \quad (43)$$

$$v_n^{1,\dots,s}(\mathbf{x}) = \frac{1}{s} \cdot \sum_{i=1}^s v_n^i(\mathbf{x}) \quad (44)$$

$$v_n^i(\mathbf{x}) = \frac{\sum_{l_n^i=0}^{\hat{l}_n^i} \varphi_n^i(l_n^i) \cdot S_{n,l_n^i}^i(\mathbf{z}_k^i) \cdot v_{\mathcal{D}_{l_n^i}^i \Xi \mathbf{z}_k^i}^i(\mathbf{x})}{\sum_{l_n^i=0}^{\hat{l}_n^i} \varphi_n^i(l_n^i) \cdot S_{n,l_n^i}^i(\mathbf{z}_k^i)} \quad (45)$$

$$v_{\mathcal{D}_{l_n^i}^i \Xi \mathbf{z}_k^i}^i(\mathbf{x}) = \frac{\sum_{W_{r,l_n^i}^i \in \mathcal{D}_{l_n^i}^i \Xi \mathbf{z}_k^i} v_{W_{r,l_n^i}^i}^i(\mathbf{x}) \cdot \prod_{\mathbf{z} \in W_{r,l_n^i}^i} D[L_{\mathbf{z}}^i]}{\sum_{W_{r,l_n^i}^i \in \mathcal{D}_{l_n^i}^i \Xi \mathbf{z}_k^i} \prod_{\mathbf{z} \in W_{r,l_n^i}^i} D[L_{\mathbf{z}}^i]} \quad (46)$$

In (43)-(46), $v_n^{1,\dots,s}(\mathbf{x})$, $v_n^i(\mathbf{x})$ and $v_{\mathcal{D}_{l_n^i}^i \Xi \mathbf{z}_k^i}^i(\mathbf{x})$ are the normalized PHDs of target number n , the i^{th} sensor and $\mathcal{D}_{l_n^i}^i \Xi \mathbf{z}_k^i$. For the sake of clarity, the proofs of (43)-(46) are given in Appendix.

3) The Multiple Fusion Process

In [33], it is proved that the value range of n can be approximated by $[n_{\min}, n_{\max}]$. Thus, (21) can be rewritten as

$$\phi = \frac{\sum_{n=n_{\min}}^{n_{\max}} n \cdot \mathcal{L}(n)}{\sum_{n=n_{\min}}^{n_{\max}} \mathcal{L}(n)} \cdot \frac{1}{N_{k|k-1} \cdot \eta} \quad (47)$$

Similarly, (28) and (43) can be given by

$$N_{k|k}^{1,\dots,s} = \sum_{n=n_{\min}}^{n_{\max}} \frac{\mathcal{L}(n)}{\sum_{n=n_{\min}}^{n_{\max}} \mathcal{L}(n)} \cdot N_n^{1,\dots,s} \quad (48)$$

$$v_{k|k}^{1,\dots,s}(\mathbf{x}) = \sum_{n=n_{\min}}^{n_{\max}} \frac{\mathcal{L}(n)}{\sum_{n=n_{\min}}^{n_{\max}} \mathcal{L}(n)} \cdot v_n^{1,\dots,s}(\mathbf{x}) \quad (49)$$

Then, the updated PHD at time k can be calculated by

$$D_{k|k}^{1,\dots,s}(\mathbf{x}) = N_{k|k}^{1,\dots,s} \cdot v_{k|k}^{1,\dots,s}(\mathbf{x}) = \sum_{n=n_{\min}}^{n_{\max}} w_n^{1,\dots,s} \cdot N_n^{1,\dots,s} \sum_{n=n_{\min}}^{n_{\max}} v_{nk|k}^{1,\dots,s}(\mathbf{x}) \quad (50)$$

To explain the process of the Two Steps PM-PHD (TS-PM-PHD) filter, (28) and (43) are rewritten as (51) and (52), as shown at the bottom of this page.

From (52), we have

$$N_{k|k}^{1,\dots,s}(\mathbf{x}) = \sum_{n \geq 0} w_n^{1,\dots,s} \cdot N_n^{1,\dots,s}(\mathbf{x}) \quad (53)$$

$$\begin{aligned} v_{k|k}^{1,\dots,s}(\mathbf{x}) &= \sum_{n \geq 0} w_n^{1,\dots,s} \cdot v_n^{1,\dots,s}(\mathbf{x}) = \sum_{n \geq 0} w_n^{1,\dots,s} \cdot \sum_{i=1}^s \frac{1}{s} \cdot \sum_{l_n^i=0}^{\hat{l}_n^i} \frac{\varphi_n^i(l_n^i) \cdot S_{n,l_n^i}^i(\mathbf{z}_k^i)}{\ell_{\mathbf{z}_k^i}^i(n)} \cdot \sum_{W_{r,l_n^i}^i \in \mathcal{D}_{l_n^i}^i \Xi \mathbf{z}_k^i} \frac{\prod_{\mathbf{z} \in W_{r,l_n^i}^i} D[L_{\mathbf{z}}^i] \cdot v_{W_{r,l_n^i}^i}^i(\mathbf{x})}{S_{n,l_n^i}^i(\mathbf{z}_k^i)} \\ &= \sum_{n \geq 0} w_n^{1,\dots,s} \cdot \sum_{i=1}^s w_n^i \cdot \sum_{l_n^i=0}^{\hat{l}_n^i} w_{\mathcal{D}_{l_n^i}^i \Xi \mathbf{z}_k^i}^i \cdot \sum_{W_{r,l_n^i}^i \in \mathcal{D}_{l_n^i}^i \Xi \mathbf{z}_k^i} w_{W_{r,l_n^i}^i}^i \cdot v_{W_{r,l_n^i}^i}^i(\mathbf{x}) \end{aligned} \quad (51)$$

$$\begin{aligned} N_{k|k}^{1,\dots,s} &= \sum_{n \geq 0} w_n^{1,\dots,s} \cdot N_n^{1,\dots,s} = \sum_{n \geq 0} w_n^{1,\dots,s} \cdot \sum_{i=1}^s \frac{1}{s} \cdot \sum_{l_n^i=0}^{\hat{l}_n^i} \frac{\varphi_n^i(l_n^i) \cdot S_{n,l_n^i}^i(\mathbf{z}_k^i)}{\ell_{\mathbf{z}_k^i}^i(n)} \cdot \sum_{W_{r,l_n^i}^i \in \mathcal{D}_{l_n^i}^i \Xi \mathbf{z}_k^i} \frac{\prod_{\mathbf{z} \in W_{r,l_n^i}^i} D[L_{\mathbf{z}}^i] \cdot N_{W_{r,l_n^i}^i}^i}{S_{n,l_n^i}^i(\mathbf{z}_k^i)} \\ &= \sum_{n \geq 0} w_n^{1,\dots,s} \cdot \sum_{i=1}^s w_n^i \cdot \sum_{l_n^i=0}^{\hat{l}_n^i} w_{\mathcal{D}_{l_n^i}^i \Xi \mathbf{z}_k^i}^i \cdot \sum_{W_{r,l_n^i}^i \in \mathcal{D}_{l_n^i}^i \Xi \mathbf{z}_k^i} w_{W_{r,l_n^i}^i}^i \cdot N_{W_{r,l_n^i}^i}^i \end{aligned} \quad (52)$$

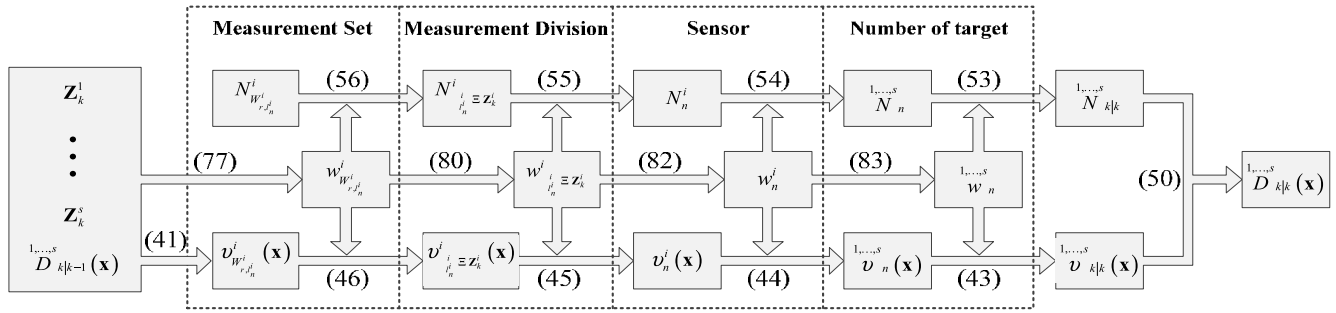


FIGURE 2. The block diagram of the TS-PM-PHD filter.

$$N_n^{1,...,s}(\mathbf{x}) = \frac{1}{s} \cdot \sum_{i=1}^s N_n^i(\mathbf{x}) \quad (54)$$

$$N_n^i(\mathbf{x}) = \frac{\sum_{l_h^i=0}^{\hat{l}_n^i} \varphi_n^i(l_h^i) \cdot S_{n,l_h^i}^i(\mathbf{Z}_k^i) \cdot N_{\mathcal{D}_{l_h^i}^i \Xi \mathbf{Z}_k^i}^i(\mathbf{x})}{\sum_{l_h^i=0}^{\hat{l}_n^i} \varphi_n^i(l_h^i) \cdot S_{n,l_h^i}^i(\mathbf{Z}_k^i)} \quad (55)$$

$$N_{\mathcal{D}_{l_h^i}^i \Xi \mathbf{Z}_k^i}^i(\mathbf{x}) = \frac{\sum_{W_{r,l_h^i}^i \in \mathcal{D}_{l_h^i}^i \Xi \mathbf{Z}_k^i} N_{W_{r,l_h^i}^i}^i(\mathbf{x}) \cdot \prod_{\mathbf{z} \in W_{r,l_h^i}^i} D[L_{\mathbf{z}}^i]}{\sum_{W_{r,l_h^i}^i \in \mathcal{D}_{l_h^i}^i \Xi \mathbf{Z}_k^i} \prod_{\mathbf{z} \in W_{r,l_h^i}^i} D[L_{\mathbf{z}}^i]} \quad (56)$$

Here, $N_n^{1,...,s}(\mathbf{x})$, N_n^i , $N_{\mathcal{D}_{l_h^i}^i \Xi \mathbf{Z}_k^i}^i$ and $N_{W_{r,l_h^i}^i}^i$ denote the target numbers of target number n , the i^{th} sensor, $\mathcal{D}_{l_h^i}^i \Xi \mathbf{z}_k^i$, and $W_{r,l_h^i}^i$, respectively. $N_{W_{r,l_h^i}^i}^i = |W_{r,l_h^i}^i|$, and $|W_{r,l_h^i}^i|$ denotes the number of measurements in $W_{r,l_h^i}^i$.

Note that the proof of (52)-(56) is similar to that of (43)-(46), and it will not be given here. Based on (51) and (52), Fig. 2 shows the block diagram of the TS-PM-PHD filter.

From (51), (52), and Fig. 2, it can be seen that the posterior PHD $D_{k|k}^{1,...,s}(\mathbf{x})$ consists of $N_{k|k}^{1,...,s}$ and $v_{k|k}^{1,...,s}(\mathbf{x})$. Both $N_{k|k}^{1,...,s}$ and $v_{k|k}^{1,...,s}(\mathbf{x})$ are the results of multiple fusion process. They are independent of each other in the calculation, but there is a one-to-one correspondence between them. The measurement sets Z_k^1, \dots, Z_k^s and the predicted PHD $D_{k|k-1}^{1,...,s}(\mathbf{x})$ don't directly affect $N_{W_{r,l_h^i}^i}^i$, $N_{\mathcal{D}_{l_h^i}^i \Xi \mathbf{Z}_k^i}^i$, N_n^i , $N_n^{1,...,s}$ and $N_{k|k}^{1,...,s}$, but rather through the weights. In the multiple fusion process, weights corresponding to the correct factors are much larger than the others. Thus, $D_{k|k}^{1,...,s}(\mathbf{x})$ can be correctly estimated by the numbers of targets and the normalized PHDs that corresponding to the correct factors.

V. SIMULATION RESULTS

The state transition model is described as

$$\mathbf{x}_k = \mathbf{F}\mathbf{x}_{k-1} + \mathbf{\Gamma}\mathbf{w}_k \quad (57)$$

Here, $\mathbf{x}_k = [x_k, \dot{x}_k, y_k, \dot{y}_k]^T$ is target state vector, x_k and y_k represent the planar position coordinates of the target, \dot{x}_k and \dot{y}_k represent their velocities, respectively. And

$$\mathbf{F} = \begin{bmatrix} 1 & T & 0 & 0 \\ 0 & 1 & 0 & 0 \\ 0 & 0 & 1 & T \\ 0 & 0 & 0 & 1 \end{bmatrix}, \mathbf{\Gamma} = \begin{bmatrix} T^2/2 & 0 \\ T & 0 \\ 0 & T^2/2 \\ 0 & T \end{bmatrix}, \mathbf{w}_k \sim \mathcal{N}\left(0, \begin{bmatrix} \sigma_w^2 & 0 \\ 0 & \sigma_w^2 \end{bmatrix}\right)$$

Here, (s) is the sampling period, and $\sigma_w = 10$ is the standard deviation of w_k .

The measurements of four sensors are given in Cartesian coordinates as follow

$$\mathbf{z}_k^l = [x_k^l \ y_k^l]^T + \mathbf{v}_k^l, l = 1, 2, 3, 4 \quad (58)$$

Here, the covariance matrix of observation noise \mathbf{v}_k^l is $\mathbf{R}_k^l = \text{diag}\{[\delta_v^2, \delta_v^2]^T\}$, $l = 1, 2, 3, 4$.

The Gaussian mixture implementations [19] of the TS-PM-PHD filter and other filters are compared in the simulation. In order to prune and merge the Gaussian components, the pruning and merging thresholds are set as $T_p = 1 \times 10^{-5}$ and $U = 4$, respectively. The maximum number of Gaussian components is $J_{\max} = 100$.

The optimal sub-pattern assignment (OSPA) [34] distance is used to evaluate the multi-target tracking performance,

$$\bar{d}_p^{(c)}(\mathbf{X}, \mathbf{Y}) = \left(\frac{1}{n} \left(\min_{\pi \in \Pi_n} \sum_{i=1}^m d^{(c)}(\mathbf{x}_i, \mathbf{y}_{\pi(i)})^p + c^p (n-m) \right) \right)^{1/p} \quad (59)$$

Here, $\mathbf{X} = \{\mathbf{x}_1, \dots, \mathbf{x}_m\}$ and $\mathbf{Y} = \{\mathbf{y}_1, \dots, \mathbf{y}_n\}$ are arbitrary finite subsets, $1 \leq p < \infty$, $c > 0$ (see [34] for the meanings of these parameters). If $m > n$, $\bar{d}_p^{(c)}(\mathbf{X}, \mathbf{Y}) = \bar{d}_p^{(c)}(\mathbf{Y}, \mathbf{X})$. In our simulations, two parameters are set as $p = 2$ and $c = 2000$, respectively. The simulation results are obtained by averaging the results of 200 Monte Carlo runs.

TABLE 2. Initial position and moving duration.

Target	Initial position (m)	Start time (s)	End time (s)
1	(-6000,0)	1	40
2	(-6000,0)	11	50
3	(0,6000)	11	50
4	(0,6000)	21	60
5	(-3000,0)	31	60
6	(4000,2000)	31	70

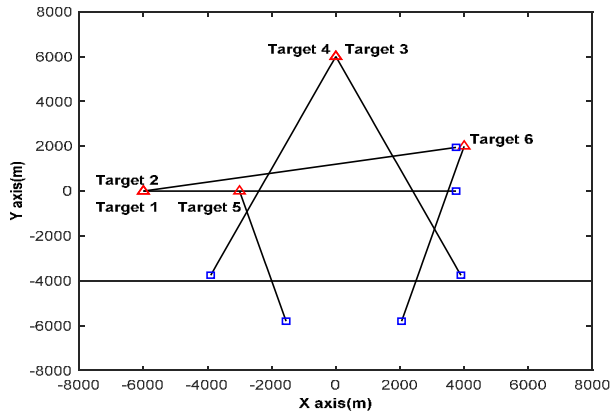


FIGURE 3. True target trajectory. ‘Δ’ – locations at which targets are born; ‘□’ – locations at which targets die.

A. EXPERIMENT

The surveillance region is set at $[-8000, 8000] \times [-8000, 8000]$ (m²), and the probability of survival is $p_{S,k} = 0.97$. Six targets with different initial positions move in the surveillance region, and the setting of targets is shown in Table 2. Fig. 3 shows the target trajectories.

The intensity of the birth Poisson RFS is described as

$$\Gamma_k(\mathbf{x}) = \sum_{j=1}^4 0.1 \mathcal{N}(\mathbf{x}; \mathbf{m}_\gamma^j, \mathbf{P}_\gamma^j) \quad (60)$$

Here, $\mathbf{P}_\gamma^1 = \mathbf{P}_\gamma^2 = \mathbf{P}_\gamma^3 = \mathbf{P}_\gamma^4 = \text{diag}[[10^4, 10^4, 10^4, 10^4]^T]$, and

$$\mathbf{m}_\gamma^1 = [-6000, 0, 0, 0]^T, \mathbf{m}_\gamma^3 = [-3000, 0, 0, 0]^T, \mathbf{m}_\gamma^2 = [0, 0, 6000, 0]^T, \mathbf{m}_\gamma^4 = [4000, 0, 2000, 0]^T.$$

The intensity of the clutter RFS is assumed to be

$$\kappa_k^i = \lambda_k^i \mathcal{U}(\mathbf{z}_k^i), i = 1, 2, 3, 4 \quad (61)$$

Here, λ_k^i is the clutter rate of the i^{th} sensor, and $\mathcal{U}(\cdot)$ is the uniform density over the surveillance region.

In this experiment, different parameters are used to verify the effectiveness of the TS-PM-PHD filter, such as the probability of detection, observation noise, and clutter rate. The setting of these parameters is given in Table 3. In Case 1-3, only one parameter is variable, and the other two parameters are fixed. Additionally, two different sensor orders are also considered here. In the first situation, the sensor with $P_{D,k} = 0.9$ is the last update sensor, while in the second situation,

TABLE 3. The setting of different parameters.

	$P_{D,k}$	λ_k	δ_v
Case 1	0.99,0.95,0.9,0.85,0.8	10	10
Case 2	0.99	10,30	10
Case 3	0.99	10	10,30

TABLE 4. The weights of Targets 1-4 at 29s.

	Target 1	Target 2	Target 3	Target 4	Sum
IC-PHD	0.1010	1.1007	1.1008	1.0943	3.3968
PM-PHD	0.1189	1.2962	1.2963	1.2887	4.0001
CM-PM-PHD	0.9220	1.0241	1.0307	1.0232	4.0000
TS-PM-PHD	0.8032	1.0662	1.0709	1.0553	3.9956

TABLE 5. The running time with different clutter rates.

	$t_{\lambda=10}$ (s)	$t_{\lambda=20}$ (s)	$t_{\lambda=30}$ (s)	Δt_1 (s)	Δt_2 (s)
IC-PHD	0.047	0.085	0.125	0.038	0.040
PM-PHD	0.050	0.084	0.123	0.034	0.039
CM-PM-PHD	0.077	0.129	0.185	0.052	0.057
TS-PM-PHD	0.124	0.224	0.373	0.100	0.148

it is the second one. The probabilities of detection of the other three sensors are $P_{D,k} = 0.99$.

The estimated number of targets, OSPA distance and mean squared error (MSE) of number of targets for different sensor orders are shown in Fig. 4(a)-(c), respectively. The Gaussian components estimated by different filters at $k = 29$ s in the first sensor order (1 \rightarrow 4) are illustrated in Fig. 5. Table 4 gives the weights of ‘Target 1-4’ at $k = 29$ s. The simulation results of different probabilities of detection, clutter rates, and observation noises are shown in and Fig. 6-Fig. 8, respectively. The running time of the IC-PHD filter, the PM-PHD filter, the CM-PM-PHD filter and the TS-PM-PHD filter is given in Table 5.

Since the TS-PM-PHD filter contains two complex multiple fusion processes, its running time is higher than other algorithms’. However, in Table 5, the TS-PM-PHD filter can still meet the real-time requirements of multi-target tracking system. In Fig. 6(a) and (b), it can be observed that the accuracy of state estimation of the CM-PM-PHD filter decreases rapidly when $P_{D,k} < 0.9$. The TS-PM-PHD filter is insensitive to a changing probability of detection and performs well in estimating the state of targets. In Fig.4, Fig. 6 - Fig. 8, the influence of different parameters and sensor orders on the TS-PM-PHD filter are lower than those of the other filters. Fig. 4 shows that the IC-PHD filter is seriously affected by the sensor order. In the IC-PHD filter, measurement set of each sensor updates the predicted PHD in turn. The updated PHD of one sensor is the predicted PHD of the next sensor. Therefore, the performance of the IC-PHD filter is mainly depends on the sensor at the end of the update order [31]. In other words, if one target is undetected by the last update

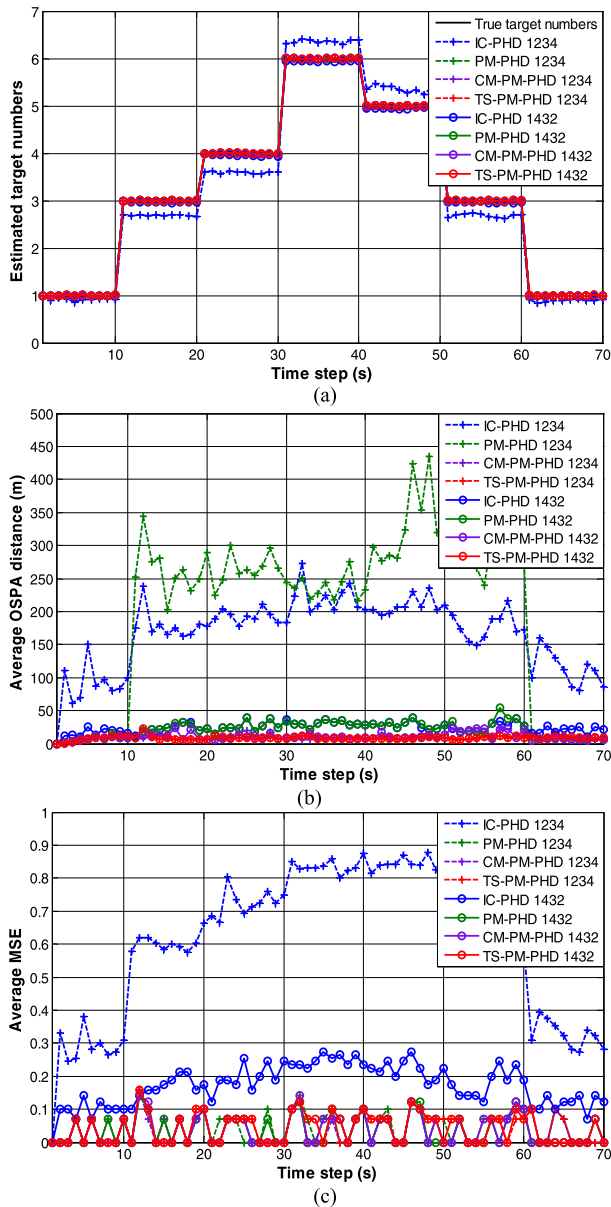


FIGURE 4. Tracking results with different updated sensor orders (a) Estimated number of targets (b) OSPA Distance (c) MSE.

sensor, it will still be undetected by the multi-sensor tracking system even if the target is detected by other sensors. In this experiment, targets are more likely to be undetected by the sensor with $P_{D,k} = 0.9$ than other sensors. Since the sensor with $P_{D,k} = 0.9$ is the last update sensor in the IC-PHD (1234) filter, targets are easily undetected by the multi-sensor system. Moreover, in the IC-PHD (1432) filter, targets undetected by the sensor with $P_{D,k} = 0.9$ will be detected by the other two sensors. Therefore, the performance of the IC-PHD (1432) filter is much better than that of the IC-PHD (1234) filter. From Fig. 5(a) and (b), we found that ‘Target 1’ is undetected by the sensor with $P_{D,k} = 0.9$ at $k = 29s$,

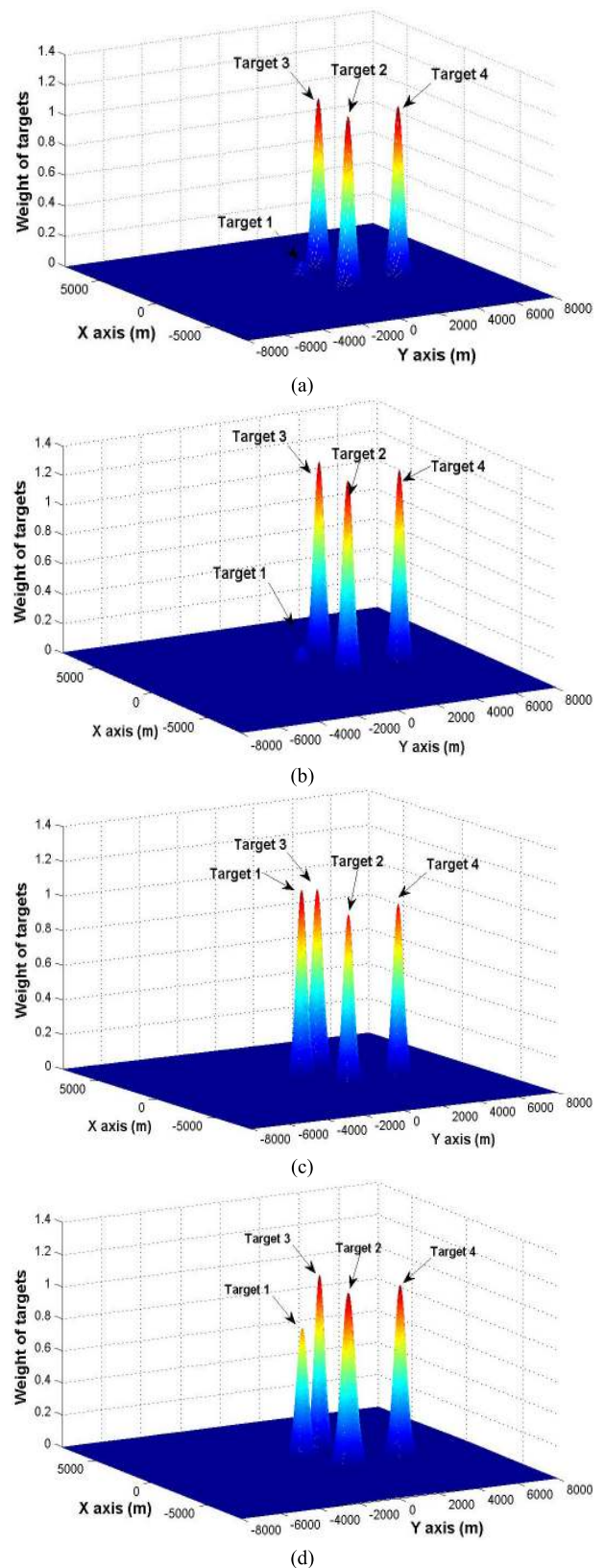


FIGURE 5. The updated Gaussian components of four filters at 29s (a) The IC-PHD filter (b) The PM-PHD filter (c) The CM-PM-PHD filter (d) The TS-PM-PHD filter.

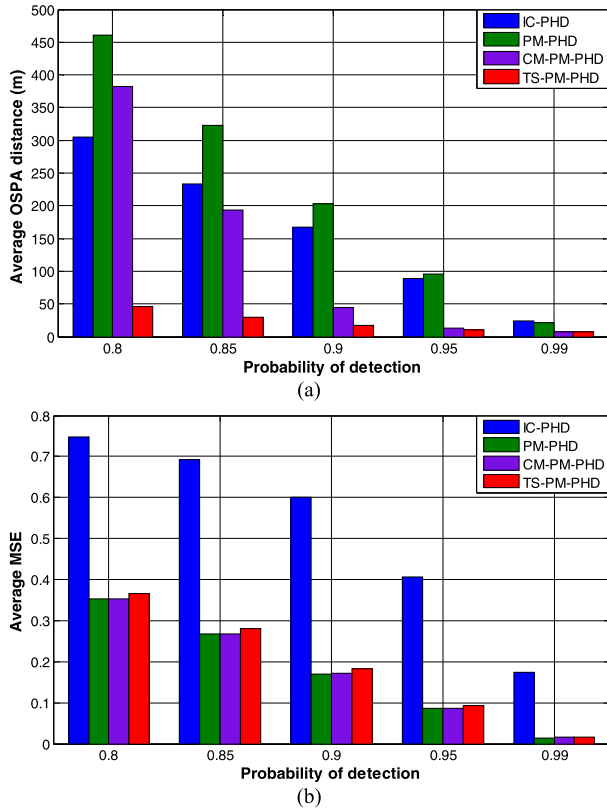


FIGURE 6. Tracking results with different probabilities of detection (a) OSPA distance (b) MSE.

and it cannot be correctly estimated by the PM-PHD filter. However, Fig. 5(c) and (d) show that the CM-PM-PHD filter and the TS-PM-PHD filter can estimate ‘Target 1’ effectively. In Table 4, the weight of ‘Target 1’ estimated by the TS-PM-PHD filter is 0.8032, and the weight of other targets is larger than 1. It seems that the TS-PM-PHD filter has the same disadvantage of the PM-PHD filter. To further explain this question, the difference between the PM-PHD filter and the TS-PM-PHD filter is discussed in detail below.

B. Difference between TS-PM-PHD and PM-PHD

Assume that there is one target, the probability of detection is independent of the state, the observation noise and the clutter rate are low. It is known by the update formula (4) of the PHD filter that the weight of targets can be approximated by

$$\begin{cases} w_{\text{target, undetected}} \approx 1 - P_{D,k} \\ w_{\text{target, detected}} \approx 1 \end{cases} \quad (62)$$

Then, for the case described in Fig. 8, the weight of ‘Target 1’ estimated by the PM-PHD filter is approximated as

$$\begin{aligned} \mathcal{W}_{\text{PM-PHD}}^{\text{Miss-detection}} &= \frac{w_{\text{target, undetected}}}{n_d \cdot w_{\text{target, detected}} + n_m \cdot w_{\text{target, undetected}}} \cdot n \end{aligned}$$

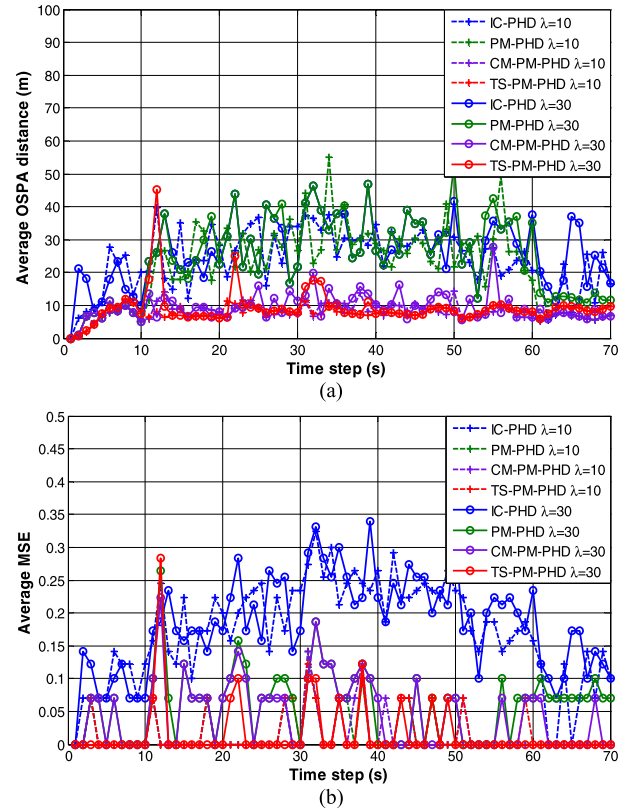


FIGURE 7. Tracking results with different clutter rates (a) OSPA distance (b) MSE.

$$\begin{aligned} &= \frac{1 - P_{D,k}}{(n - 1) \cdot 1 + 1 \cdot (1 - P_{D,k})} \cdot n \\ &= \frac{1 - P_{D,k}}{n - P_{D,k}} \cdot n \end{aligned} \quad (63)$$

The weights of ‘Target 2’ - ‘Target 4’ estimated by the PM-PHD filter are approximated as

$$\begin{aligned} \mathcal{W}_{\text{PM-PHD}}^{\text{Miss-detection}} &= \frac{w_{\text{target, detected}}}{n_d \cdot w_{\text{target, detected}} + n_m \cdot w_{\text{target, undetected}}} \cdot n \\ &= \frac{1}{(n - 1) \cdot 1 + 1 \cdot (1 - P_{D,k})} \cdot n \\ &= \frac{1}{n - P_{D,k}} \cdot n \end{aligned} \quad (64)$$

The weight of ‘Target 1’ estimated by the TS-PM-PHD filter is approximated as

$$\begin{aligned} \mathcal{W}_{\text{TS-PM-PHD}}^{\text{Detection}} &= \frac{w_{\text{target, detected}}}{n_d \cdot w_{\text{target, detected}} + n_m \cdot \frac{w_{\text{target, undetected}} \cdot s_m + w_{\text{target, detected}} \cdot s_d}{s}} \cdot n \\ &= \frac{1}{(n - 1) + \frac{(1 - P_{D,k}) + (s - 1)}{s}} \cdot n = \frac{s}{n \cdot s - P_{D,k}} \cdot n \end{aligned} \quad (65)$$

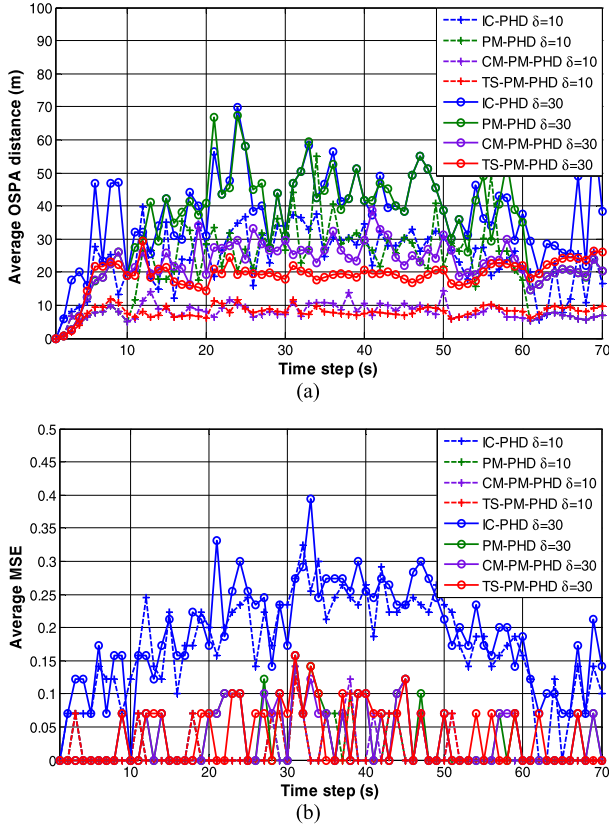


FIGURE 8. Tracking results with different observation noises (a) OSPA distance (b) MSE.

The weights of ‘Target 2’ - ‘Target 4’ estimated by the TS-PM-PHD filter are approximated as

$$\begin{aligned} & \mathcal{W}_{\text{TS-PM-PHD}}^{\text{Miss-detection}} \\ &= \frac{w_{\text{target, undetected}} \cdot s_m + w_{\text{target, detected}} \cdot s_d}{s} \\ &= \frac{n_d \cdot w_{\text{target, detected}} + n_m \cdot \frac{w_{\text{target, undetected}} s_m + w_{\text{target, detected}} s_d}{s}}{(1-P_{D,k})+(s-1)} \cdot n \\ &= \frac{s - P_{D,k}}{(n-1) + \frac{(1-P_{D,k})+(s-1)}{s}} \cdot n = \frac{s - P_{D,k}}{n \cdot s - P_{D,k}} \cdot n \quad (66) \end{aligned}$$

Here, n_d and n_m are the numbers of targets detected and undetected, and $n_m = 1, n_d + n_m = n$ is the number of targets, and $n = 4$. s_d and s_m denote the numbers of sensors which detect and miss detect the target, and $s_m = 1, s_d + s_m = s$. s is the number of sensors, and $s = 4$. $P_{D,k}$ is the probability of detection of the last updated sensor. Fig. 9 shows the effects of $P_{D,k}$ on (63) - (65).

In Fig. 9, when $P_{D,k} = 0.9$, the weights of targets calculated by (63) - (65) are basically consistent with that in Table 5. It can be seen that $P_{D,k}$ has the greatest impact on $\mathcal{W}_{\text{PM-PHD}}^{\text{Miss-detection}}$, and the second impact on $\mathcal{W}_{\text{PM-PHD}}^{\text{Detection}}$. Contrarily, the impact of $P_{D,k}$ on $\mathcal{W}_{\text{TS-PM-PHD}}^{\text{Miss-detection}}$ and $\mathcal{W}_{\text{TS-PM-PHD}}^{\text{Detection}}$ is relatively small.

No matter what the value of $P_{D,k}$ is, ‘Target 1’ can always be estimated by

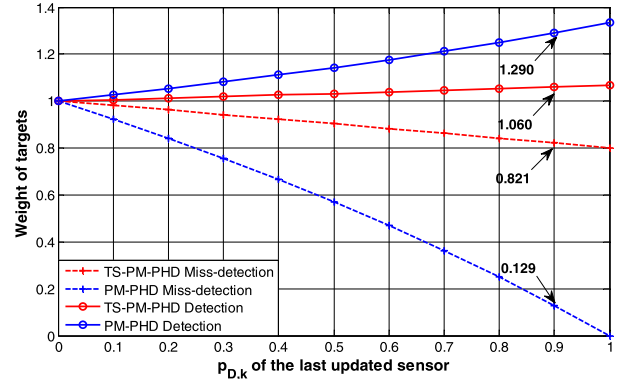


FIGURE 9. Weight of targets estimated by the PM-PHD filter and the TS-PM-PHD filter.

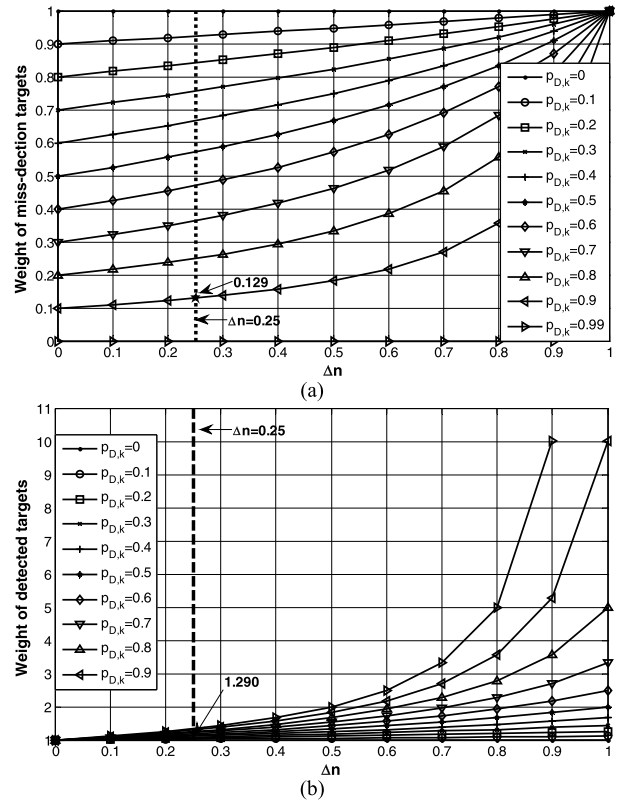


FIGURE 10. The curves of weights of targets estimated by the PM-PHD filter with different Δn . (a) Undetected target. (b) Detected target.

the TS-PM-PHD filter. Fig. 9 only considers the situation that single target is undetected by the last updated sensor. The following part will further study the situation that multiple targets are undetected by multiple sensors. To facilitate discussion, the probabilities of detections of all sensors are assumed to be the same and denoted by $\bar{P}_{D,k}$. Then, the weights estimated by the PM-PHD filter of the undetected targets can be approximated as

$$\mathcal{W}_{\text{PM-PHD}}^{\text{Miss-detection}} = \frac{(1 - \bar{P}_{D,k})^{s_m}}{n_d + n_m \cdot (1 - \bar{P}_{D,k})^{s_m}} \cdot n \quad (67)$$

TABLE 6. The effect of different variables on the weights of targets.

	$n_d \uparrow$	$n_m \uparrow$	$n \uparrow$	$s_d \uparrow$	$s_m \uparrow$	$s \uparrow$	$\bar{P}_{D,k} \uparrow$
$W_{\text{PM-PHD}}$ Miss-detection	↓	↑	↓	—	—	—	↓
$W_{\text{PM-PHD}}$ Detection	↑	↓	↑	—	—	—	↑
$W_{\text{TS-PM-PHD}}$ Miss-detection	↓	↑	↓	↑	↓	↑	↓
$W_{\text{TS-PM-PHD}}$ Detection	↑	↓	↑	↓	↑	↓	↑

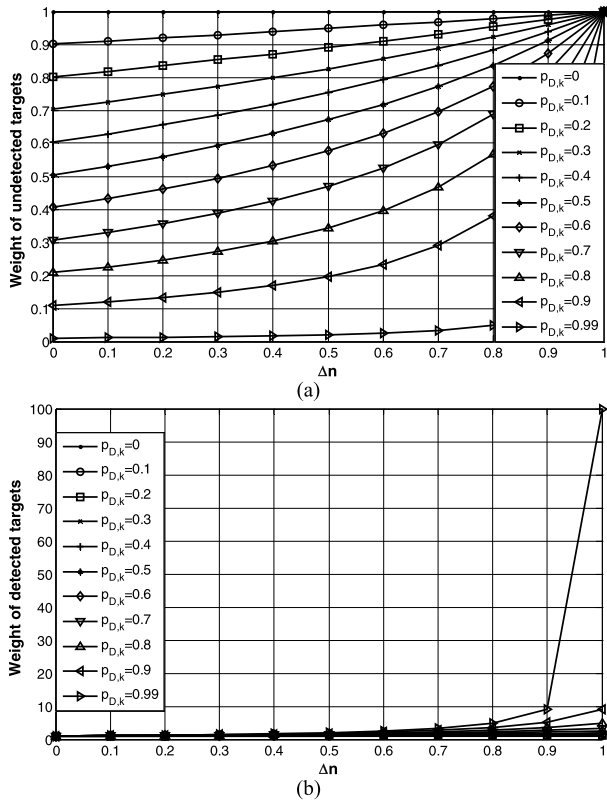


FIGURE 11. The curves of weights of targets estimated by the TS-PM-PHD filter with different Δn ($\Delta s = 1$). (a) Undetected target (b) Detected target.

Note that the PM-PHD filter is an improved IC-PHD filter. It is mainly determined by the last updated sensor that whether one target can be estimated or not. Therefore, n_d and n_m in (67) are the numbers of targets detected and undetected by the last updated sensor respectively, and $n_d + n_m = n$. s_m is the number of sensors which miss detect the target continuously in reverse order. (67) indicates that $w_{\text{PM-PHD}}$ Miss-detection decreases rapidly and becomes extremely inaccurate with the increase of s_m ($s_m \ll s$). Since the PM-PHD filter with larger s_m performs poor, s_m is set to be 1 here. Then, (67) can be rewritten as

$$\begin{aligned}
 W_{\text{PM-PHD}}^{\text{Miss-Detection}} &= \frac{1 - \bar{P}_{D,k}}{n_d + n_m \cdot (1 - \bar{P}_{D,k})} \cdot n \\
 &= \frac{1 - \bar{P}_{D,k}}{n - n_m \cdot \bar{P}_{D,k}} \cdot n \quad (68)
 \end{aligned}$$

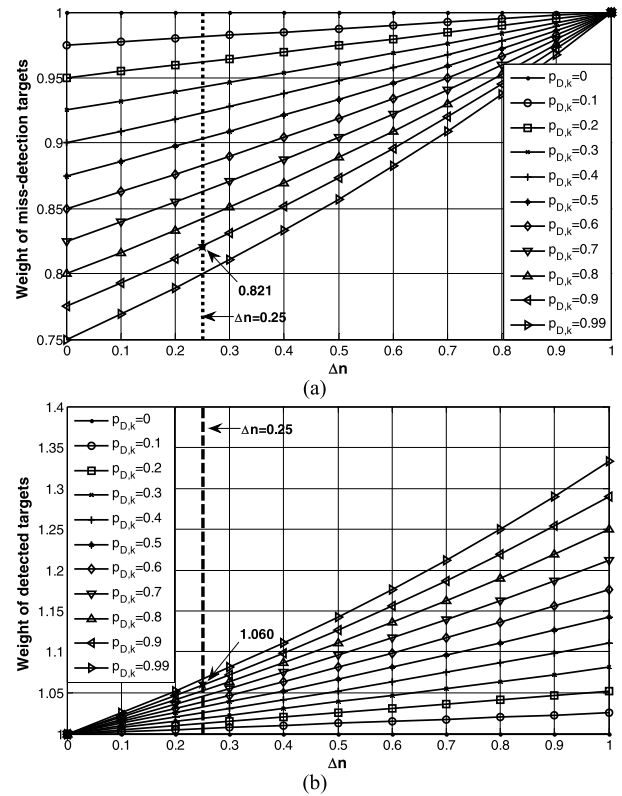


FIGURE 12. The curves of weights of targets estimated by the TS-PM-PHD filter with different Δn ($\Delta s = 0.25$). (a) Undetected target. (b) Detected target.

Similarly, the weight estimated by the PM-PHD filter of the detected targets can be approximated as

$$\begin{aligned}
 W_{\text{PM-PHD}}^{\text{Detection}} &= \frac{1}{n_d + n_m \cdot (1 - \bar{P}_{D,k})^{s_m}} \cdot n \\
 &= \frac{1}{n - n_m \cdot \bar{P}_{D,k}} \cdot n \quad (69)
 \end{aligned}$$

For the TS-PM-PHD filter, the weights of the undetected and detected targets can be approximated as

$$\begin{aligned}
 W_{\text{TS-PM-PHD}}^{\text{Miss-detection}} &= \frac{(1 - \bar{P}_{D,k})^{s_m + s_d}}{s} \cdot n \\
 &= \frac{s - s_m \cdot \bar{P}_{D,k}}{n \cdot s - n_m \cdot s_m \cdot \bar{P}_{D,k}} \cdot n \quad (70)
 \end{aligned}$$

$$\begin{aligned}
 W_{\text{TS-PM-PHD}}^{\text{Detection}} &= \frac{1}{n_d + n_m \cdot \frac{(1 - \bar{P}_{D,k})^{s_m + s_d}}{s}} \cdot n \\
 &= \frac{s}{n \cdot s - n_m \cdot s_m \cdot \bar{P}_{D,k}} \cdot n \quad (71)
 \end{aligned}$$

In (70) and (71), n_d denotes the number of targets detected by all sensors, n_m denotes the number of targets undetected by at least one sensor, and $n_d + n_m = n$. For a target, s_d and s_m denote the numbers of sensors which detect and miss detect the target, respectively, and

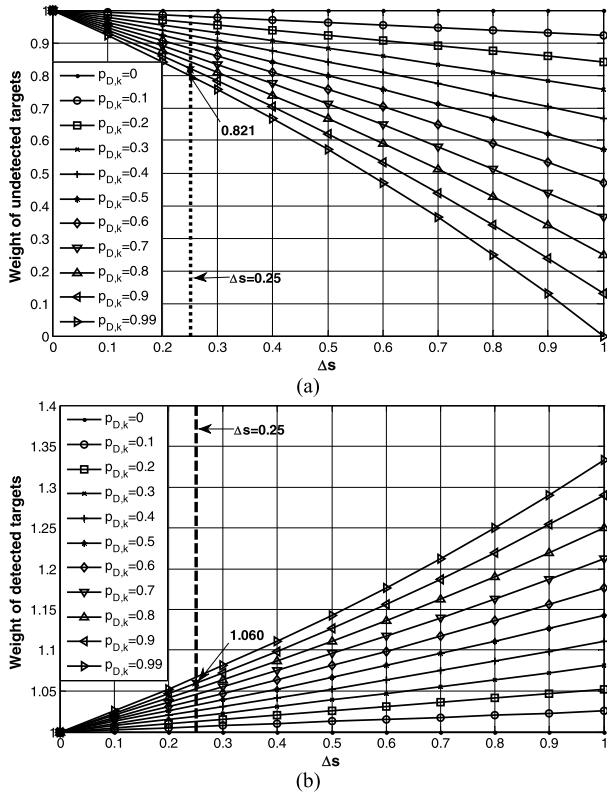


FIGURE 13. The curves of weights of targets estimated by the TS-PM-PHD filter with different Δs ($\Delta n = 0.25$). (a) Undetected target. (b) Detected target.

$s_d + s_m = s$. Table 6 gives the influences of variables ($n_d, n_m, n, s_d, s_m, s, \bar{P}_{D,k}$) in (68)-(71).

In Table 6, \uparrow and \downarrow denote increase and decrease respectively, and $—$ denotes unchanged. To illustrate Table 6 intuitively, (68)-(71) can be rewritten by

$$\mathcal{W}_{\text{PM-PHD}}^{\text{Miss-detection}} = \frac{1 - \bar{P}_{D,k}}{1 - \Delta n \cdot \bar{P}_{D,k}} \quad (72)$$

$$\mathcal{W}_{\text{PM-PHD}}^{\text{Detection}} = \frac{1}{1 - \Delta n \cdot \bar{P}_{D,k}} \quad (73)$$

$$\mathcal{W}_{\text{TS-PM-PHD}}^{\text{Miss-detection}} = \frac{1 - \Delta s \cdot \bar{P}_{D,k}}{1 - \Delta n \cdot \Delta s \cdot \bar{P}_{D,k}} \quad (74)$$

$$\mathcal{W}_{\text{TS-PM-PHD}}^{\text{Detection}} = \frac{1}{1 - \Delta n \cdot \Delta s \cdot \bar{P}_{D,k}} \quad (75)$$

Here, $\Delta n = n_m/n$ denotes the ratio of undetected targets in all targets, and $\Delta s = s_m/s$ denotes the ratio of the sensors which miss detect targets in all sensors. The curves of weights of targets estimated by the PM-PHD filter and the TS-PM-PHD filter with Δn and Δs are shown in Fig. 10- Fig. 13.

As shown in Fig. 10(a), the weight of the undetected targets increases with the increase of Δn , and the PM-PHD filter begins to estimate the undetected targets correctly. However, in Fig. 10(b), with the increase of Δn , the weight of the detected targets increases much faster than that of the undetected targets. And thus the PM-PHD filter may estimate

multiple false targets. Fig. 10 and Fig. 11 show that the performance of the TS-PM-PHD filter is the same as that of the PM-PHD filter at the extreme case of $\Delta s = 1$. (74) and (75) indicate that the performance of the TS-PM-PHD filter is improved with the decrease of Δs . In Fig. 12, when $\Delta s = 0.25$, the TS-PM-PHD filter can estimate the weights of the undetected targets and the detected targets effectively. Furthermore, false targets are not estimated by the TS-PM-PHD filter. In Fig. 13, the undetected targets cannot be estimated by the TS-PM-PHD filter in a few cases ($\Delta s \geq 0.6$ and $P_{D,k} \geq 0.7$), but the weight of the detected target is still within a normal range. Therefore, targets can be estimated correctly by the TS-PM-PHD filter in most situations.

VI. CONCLUSION

In this paper, an improved version of the PM-PHD filter is proposed to modify state estimation. The proposed algorithm is dependent on the combination of factors, instead of the measurements. Firstly, the number of targets and normalized PHDs of all combinations are fused, respectively. Then, the state and the number of targets can be estimated by the fusion results, simultaneously. Theoretical analysis and simulation show that the proposed method is insensitive to the sensor parameters and performs well in both the state estimation and cardinality estimation. Some assumptions have been made to facilitate the implementation of the TS-PM-PHD filter, but these assumptions limit the application of the algorithm. In the future work, the proposed method will be used to deal with more practical engineering problems, such as partially/non-overlapped FoV [35] and heterogeneous sensor networks [36]. Therefore, we will take the detection probability, FoV, and observation noise of sensors into consideration when designing (40) and (44).

APPENDIX

In (38), each combination consists of n, l_n^1, \dots, l_n^s and $W_{r,l_n^1}^1, \dots, W_{r,l_n^s}^s$. If n, l_n^1, \dots, l_n^s and $W_{r,l_n^1}^1, \dots, W_{r,l_n^{i'-1}}^{i'-1}, W_{r,l_n^{i'+1}}^{i'+1}, \dots, W_{r,l_n^s}^s$ are given, the measurement subsets in $\mathcal{D}_{l_n^{i'}}^{i'} \Xi \mathcal{Z}_k^{i'}$ will generate $C_m^{l_n^{i'}}$ combinations. Then, the fusion result of the $C_m^{l_n^{i'}}$ combinations is computed by (76), as shown at the top of the next page.

$$\begin{aligned} u_{\mathcal{D}_{l_n^{i'}}^{i'} \Xi \mathcal{Z}_k^{i'}}^{i'}(\mathbf{x}) &= \frac{\sum_{W_{r,l_n^{i'}}^{i'} \in \mathcal{D}_{l_n^{i'}}^{i'} \Xi \mathcal{Z}_k^{i'}} v_{W_{r,l_n^{i'}}^{i'}}^i(\mathbf{X}) \cdot \prod_{\mathbf{z} \in W_{r,l_n^{i'}}^{i'}} D[L_{\mathbf{z}}^{i'}]}{\sum_{W_{r,l_n^{i'}}^{i'} \in \mathcal{D}_{l_n^{i'}}^{i'} \Xi \mathcal{Z}_k^{i'}} \prod_{\mathbf{z} \in W_{r,l_n^{i'}}^{i'}} D[L_{\mathbf{z}}^{i'}]} \\ &= \sum_{W_{r,l_n^{i'}}^{i'} \in \mathcal{D}_{l_n^{i'}}^{i'} \Xi \mathcal{Z}_k^{i'}} w_{W_{r,l_n^{i'}}^{i'}}^i \cdot v_{W_{r,l_n^{i'}}^{i'}}^i(\mathbf{X}) \quad (77) \end{aligned}$$

$$\begin{aligned}
 & \Psi_{n, l_n^1, \dots, l_n^s, W_{r, l_n^1}^1, \dots, W_{r, l_n^{i'-1}}^{i'-1}, W_{r, l_n^{i'+1}}^{i'+1}, \dots, W_{r, l_n^s}^s, \mathcal{D}_{l_n^i}^{i'} \Xi \mathbf{Z}_k^{i'}} \\
 &= \frac{\binom{1, \dots, s}{N_{k|k-1} \cdot \eta}^n}{n! \cdot \sum_{n \geq 0} \mathcal{L}(n)} \cdot \prod_{i=1}^s \varphi_n^i(l_n^i) \cdot \prod_{\substack{1 \leq i \leq s \\ i \neq i'}} \prod_{\mathbf{z} \in W_{r, l_n^i}^i} D[L_{\mathbf{z}}^i] \cdot \\
 & \times \frac{1}{s} \cdot \left(\sum_{\substack{W_{r, l_n^i}^{i'} \in \mathcal{D}_{l_n^i}^{i'} \Xi \mathbf{Z}_k^{i'} \\ \mathbf{z} \in W_{r, l_n^i}^{i'}}} \prod_{\mathbf{z} \in W_{r, l_n^i}^{i'}} D[L_{\mathbf{z}}^{i'}] \cdot v_{W_{r, l_n^i}^{i'}}^i(\mathbf{x}) + \sum_{\substack{1 \leq i \leq s \\ i \neq i'}} s_{W_{r, l_n^i}^i}^i(\mathbf{x}) + \sum_{W_{r, l_n^i}^{i'} \in \mathcal{D}_{l_n^i}^{i'} \Xi \mathbf{Z}_k^{i'}} v_{W_{r, l_n^i}^{i'}}^i(\mathbf{x}) \cdot \prod_{\mathbf{z} \in W_{r, l_n^i}^{i'}} D[L_{\mathbf{z}}^{i'}] \right) \\
 &= \frac{\binom{1, \dots, s}{N_{k|k-1} \cdot \eta}^n}{n! \cdot \sum_{n \geq 0} \mathcal{L}(n)} \cdot \prod_{i=1}^s \varphi_n^i(l_n^i) \cdot \prod_{\substack{1 \leq i \leq s \\ i \neq i'}} \prod_{\mathbf{z} \in W_{r, l_n^i}^i} D[L_{\mathbf{z}}^i] \cdot \mathcal{S}_{n, l_n^i}^{i'}(\mathbf{Z}_k^{i'}) \cdot \frac{\left(\sum_{\substack{1 \leq i \leq s \\ i \neq i'}} v_{W_{r, l_n^i}^i}^i(\mathbf{x}) + v_{\mathcal{D}_{l_n^i}^{i'} \Xi \mathbf{Z}_k^{i'}}^i(\mathbf{x}) \right)}{s} \quad (76)
 \end{aligned}$$

$$\begin{aligned}
 & \Psi_{n, l_n^1, \dots, l_n^{i'-1}, l_n^{i'+1}, \dots, l_n^s, \hat{l}_n^{i'}} \\
 &= \frac{\binom{1, \dots, s}{N_{k|k-1} \cdot \eta}^n}{n! \cdot \sum_{n \geq 0} \mathcal{L}(n)} \cdot \prod_{\substack{1 \leq i \leq s \\ i \neq i'}} \varphi_n^i(l_n^i) \cdot \mathcal{S}_{n, l_n^i}^i(\mathbf{Z}_k^i) \cdot \\
 & \times \frac{1}{s} \cdot \left(\sum_{\hat{l}_n^{i'}=0}^{\hat{l}_n^{i'}} \varphi_n^{i'}(l_n^{i'}) \cdot \mathcal{S}_{n, l_n^{i'}}^{i'}(\mathbf{Z}_k^{i'}) \cdot \sum_{\substack{1 \leq i \leq s \\ i \neq i'}} v_{\mathcal{D}_{l_n^i}^i \Xi \mathbf{Z}_k^i}^i(\mathbf{X}) + \sum_{\hat{l}_n^{i'}=0}^{\hat{l}_n^{i'}} \varphi_n^{i'}(l_n^{i'}) \cdot \mathcal{S}_{n, l_n^{i'}}^{i'}(\mathbf{Z}_k^{i'}) \cdot v_{\mathcal{D}_{l_n^i}^{i'} \Xi \mathbf{Z}_k^{i'}}^i(\mathbf{X}) \right) \\
 &= \frac{\binom{1, \dots, s}{N_{k|k-1} \cdot \eta}^n}{n! \cdot \sum_{n \geq 0} \mathcal{L}(n)} \cdot \prod_{\substack{1 \leq i \leq s \\ i \neq i'}} \varphi_n^i(l_n^i) \cdot \mathcal{S}_{n, l_n^i}^i(\mathbf{Z}_k^i) \cdot \ell_{\mathbf{Z}_k^i}^{i'}(n) \cdot \frac{\left(\sum_{\substack{1 \leq i \leq s \\ i \neq i'}} v_{\mathcal{D}_{l_n^i}^i \Xi \mathbf{Z}_k^i}^i(\mathbf{X}) + v_n^i(\mathbf{X}) \right)}{s} \quad (79)
 \end{aligned}$$

In (77), the weighted sum of $v_{W_{r, l_n^i}^i}^i(\mathbf{x})$ is $v_{\mathcal{D}_{l_n^i}^{i'} \Xi \mathbf{Z}_k^{i'}}^i(\mathbf{x})$, and $v_{\mathcal{D}_{l_n^i}^{i'} \Xi \mathbf{Z}_k^{i'}}^i(\mathbf{x})$ is the normalized PHD of $\mathcal{D}_{l_n^i}^{i'} \Xi \mathbf{Z}_k^{i'}$. $w_{r, l_n^i}^i$ is the weight of $v_{W_{r, l_n^i}^i}^i(\mathbf{x})$.

When $i' = 1, \dots, s$, the fusion result of the combinations that have the same factors n, l_n^1, \dots, l_n^s can be obtained by

$$\begin{aligned}
 & \Psi_{n, l_n^1, \dots, l_n^s, \mathcal{D}_{l_n^1}^1 \Xi \mathbf{Z}_k^1, \dots, \mathcal{D}_{l_n^s}^s \Xi \mathbf{Z}_k^s} \\
 &= \frac{\binom{1, \dots, s}{N_{k|k-1} \cdot \eta}^n}{n! \cdot \sum_{n \geq 0} \mathcal{L}(n)} \cdot \prod_{i=1}^s \varphi_n^i(l_n^i) \cdot \\
 & \times \mathcal{S}_{n, l_n^i}^i(\mathbf{Z}_k^i) \cdot \frac{\sum_{i=1}^s v_{\mathcal{D}_{l_n^i}^i \Xi \mathbf{Z}_k^i}^i(\mathbf{x})}{s} \quad (78)
 \end{aligned}$$

If factors n and $l_n^1, \dots, l_n^{i'-1}, l_n^{i'+1}, \dots, l_n^s$ are given, the number of detected targets $l_n^{i'}$ of the i' th sensor will generate $\hat{l}_n^{i'}$ combinations. Then, the fusion result of these combinations is computed by (79), as shown at the top of this page, and (80).

$$\begin{aligned}
 v_n^{i'}(\mathbf{x}) &= \frac{\sum_{\hat{l}_n^{i'}=0}^{\hat{l}_n^{i'}} \varphi_n^{i'}(l_n^{i'}) \cdot \mathcal{S}_{n, l_n^{i'}}^{i'}(\mathbf{Z}_k^{i'}) \cdot v_{\mathcal{D}_{l_n^i}^{i'} \Xi \mathbf{Z}_k^{i'}}^i(\mathbf{x})}{\sum_{\hat{l}_n^{i'}=0}^{\hat{l}_n^{i'}} \varphi_n^{i'}(l_n^{i'}) \cdot \mathcal{S}_{n, l_n^{i'}}^{i'}(\mathbf{Z}_k^{i'})} \\
 &= \sum_{\hat{l}_n^{i'}=0}^{\hat{l}_n^{i'}} w_{\mathcal{D}_{l_n^i}^{i'} \Xi \mathbf{Z}_k^{i'}}^{i'} \cdot v_{\mathcal{D}_{l_n^i}^{i'} \Xi \mathbf{Z}_k^{i'}}^i(\mathbf{x}) \quad (80)
 \end{aligned}$$

In (80), the weighted sum of $v_{\mathcal{D}_{i_h}^{i'} \Xi z_k^{i'}}(\mathbf{x})$ is $v_n^{i'}(\mathbf{x})$, and $v_n^{i'}(\mathbf{x})$ is the normalized PHD of the i' th sensor. $w_{\mathcal{D}_{i_h}^{i'} \Xi z_k^{i'}}^{i'}$ is the weight of $v_{\mathcal{D}_{i_h}^{i'} \Xi z_k^{i'}}(\mathbf{x})$.

When $i' = 1, \dots, s$, the fusion result of the combinations that have the same factor n can be obtained by

$$\begin{aligned} \Psi_{n, \hat{1}_n^1, \dots, \hat{1}_n^s} &= \frac{\binom{1, \dots, s}{N_{k|k-1} \cdot \eta}}{n! \cdot \sum_{n \geq 0} \mathcal{L}(n)} \cdot \prod_{i=1}^s \ell_{z_k^i}^i(n) \cdot v_n^{1, \dots, s}(\mathbf{x}) \\ &= \frac{1, \dots, s}{w_n} \cdot v_n^{1, \dots, s}(\mathbf{x}) \end{aligned} \quad (81)$$

$$v_n^{1, \dots, s}(\mathbf{x}) = \sum_{i=1}^s \frac{1}{S} \cdot v_n^i(\mathbf{x}) = \sum_{i=1}^s w_n^i \cdot v_n^i(\mathbf{x}) \quad (82)$$

Then, for $n \geq 0$, we have

$$\begin{aligned} v_{k|k}^{1, \dots, s}(\mathbf{x}) &= \sum_{n \geq 0} \Psi_{n, \hat{1}_n^1, \dots, \hat{1}_n^s} \\ &= \frac{1, \dots, s}{w_n} \cdot v_n^{1, \dots, s}(\mathbf{x}) \end{aligned} \quad (83)$$

The proofs of (43)-(46) are complete.

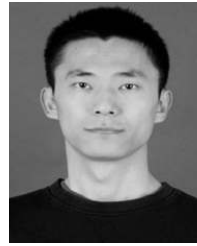
REFERENCES

- [1] Y. Bar-Shalom and X.-R. Li, *Multitarget-Multisensor Tracking: Principles and Techniques*, vol. 19. Storrs, CT, USA: YBS, 1995.
- [2] S. Blackman and R. Popoli, *Design and Analysis of Modern Tracking Systems*. New York, NY, USA: Artech House, 1999.
- [3] Y. Bar-Shalom, P. K. Willett, and X. Tian, *Tracking and Data Fusion*. Storrs, CT, USA: YBS, 2011.
- [4] T. Fortmann, Y. Bar-Shalom, and M. Scheffe, "Sonar tracking of multiple targets using joint probabilistic data association," *IEEE J. Ocean. Eng.*, vol. OE-8, no. 3, pp. 173–184, Jul. 1983.
- [5] R. Danchick and G. E. Newnam, "Reformulating Reid's MHT method with generalised Murty K-best ranked linear assignment algorithm," *IEE Proc.-Radar, Sonar Navigat.*, vol. 153, no. 1, pp. 13–22, Feb. 2006.
- [6] S. S. Blackman, "Multiple hypothesis tracking for multiple target tracking," *IEEE Aerosp. Electron. Syst. Mag.*, vol. 19, no. 1, pp. 5–18, Jan. 2004.
- [7] L.-Q. Li and W.-X. Xie, "Intuitionistic fuzzy joint probabilistic data association filter and its application to multitarget tracking," *Signal Process.*, vol. 96, pp. 433–444, Mar. 2014.
- [8] X. Jiang, K. Harishan, R. Tharmarasa, T. Kirubarajan, and T. Thayaparan, "Integrated track initialization and maintenance in heavy clutter using probabilistic data association," *Signal Process.*, vol. 94, pp. 241–250, Jan. 2014.
- [9] R. P. S. Mahler, "Random-set approach to data fusion," *Proc. SPIE*, vol. 2234, Jul. 1994, pp. 287–295.
- [10] B. Yang, J. Wang, C. Yuan, J. Thiyaalingam, and T. Kirubarajan, "Multi-object Bayesian filters with amplitude information in clutter background," *Signal Process.*, vol. 152, pp. 22–34, Nov. 2018.
- [11] R. P. S. Mahler, "Multitarget Bayes filtering via first-order multitarget moments," *IEEE Trans. Aerosp. Electron. Syst.*, vol. 39, no. 4, pp. 1152–1178, Oct. 2003.
- [12] Z. Liu, S. Chen, H. Wu, and K. Chen, "Robust student's t mixture probability hypothesis density filter for multi-target tracking with heavy-tailed noises," *IEEE Access*, vol. 6, pp. 39208–39219, Jul. 2018.
- [13] R. Mahler, "PHD filters of higher order in target number," *IEEE Trans. Aerosp. Electron. Syst.*, vol. 43, no. 4, pp. 1523–1543, Oct. 2007.
- [14] M. Wang, H. Ji, Y. Zhang, and X. Hu, "A student's t mixture cardinality-balanced multi-target multi-Bernoulli filter with heavy-tailed process and measurement noises," *IEEE Access*, vol. 6, pp. 51098–51109, Sep. 2018.
- [15] B.-T. Vo, B.-N. Vo, and A. Cantoni, "The cardinality balanced multi-target multi-Bernoulli filter and its implementations," *IEEE Trans. Signal Process.*, vol. 57, no. 2, pp. 409–423, Feb. 2009.
- [16] B.-N. Vo, S. Singh, and A. Doucet, "Sequential Monte Carlo implementation of the PHD filter for multi-target tracking," in *Proc. 6th Int. Conf. Inf. Fusion (FUSION)*, Jul. 2003, pp. 792–799.
- [17] B.-N. Vo, S. Singh, and A. Doucet, "Sequential Monte Carlo methods for multitarget filtering with random finite sets," *IEEE Trans. Aerosp. Electron. Syst.*, vol. 41, no. 4, pp. 1224–1245, Oct. 2005.
- [18] B.-N. Vo and W.-K. Ma, "A closed-form solution for the probability hypothesis density filter," in *Proc. 7th Int. Conf. Inf. Fusion (FUSION)*, Jul. 2005, pp. 856–863.
- [19] B. N. Vo and W. K. Ma, "The Gaussian mixture probability hypothesis density filter," *IEEE Trans. Signal Process.*, vol. 54, no. 11, pp. 4091–4104, Nov. 2006.
- [20] R. P. S. Mahler, *Statistical Multisource-Multitarget Information Fusion*. Boston, MA, USA: Artech House, 2007.
- [21] B. Ristic, B.-T. Vo, B.-N. Vo, and A. Farina, "A tutorial on Bernoulli filters: Theory, implementation and applications," *IEEE Trans. Signal Process.*, vol. 61, no. 13, pp. 3406–3430, Jul. 2013.
- [22] B.-T. Vo and B.-N. Vo, "A random finite set conjugate prior and application to multi-target tracking," in *Proc. 7th Int. Conf. Intell. Sensors Sensor Netw. Inf. Process. (ISSNIP)*, Dec. 2011, pp. 431–436.
- [23] B.-T. Vo and B.-N. Vo, "Labeled random finite sets and multi-object conjugate priors," *IEEE Trans. Signal Process.*, vol. 61, no. 13, pp. 3460–3475, Jul. 2013.
- [24] S. Reuter, B.-T. Vo, B.-N. Vo, and K. Dietmayer, "Multi-object tracking using labeled multi-Bernoulli random finite sets," in *Proc. 17th Int. Conf. Inf. Fusion (FUSION)*, Jul. 2014, pp. 1–8.
- [25] S. Reuter, B. T. Vo, B. N. Vo, and K. Dietmayer, "The labeled multi-Bernoulli filter," *IEEE Trans. Signal Process.*, vol. 62, no. 12, pp. 3246–3260, Dec. 2014.
- [26] B. N. Vo, B. T. Vo, and D. Phung, "Labeled random finite sets and the Bayes multi-target tracking filter," *IEEE Trans. Signal Process.*, vol. 62, no. 24, pp. 6554–6567, Dec. 2014.
- [27] B. Khaleghi, A. Khamis, F. O. Karray, and S. N. Razavi, "Multisensor data fusion: A review of the state-of-the-art," *Inf. Fusion*, vol. 14, no. 1, pp. 28–44, Jan. 2013.
- [28] T. Li, J. Prieto, H. Fan, and J. M. Corchado, "A robust multi-sensor PHD filter based on multi-sensor measurement clustering," *IEEE Commun. Lett.*, vol. 22, no. 10, pp. 2064–2067, Oct. 2018.
- [29] R. Mahler, "The multisensor PHD filter: I. General solution via multitarget calculus," *Proc. SPIE*, vol. 7336, May 2009, Art. no. 73360E.
- [30] S. Nannuru, M. Coates, M. Rabbat, and S. Blouin, "General solution and approximate implementation of the multisensor multitarget CPHD filter," in *Proc. IEEE Int. Conf. Acoust. Speech Signal Process. (ICASSP)*, Apr. 2015, pp. 4055–4059.
- [31] S. Nagappa and D. E. Clark, "On the ordering of the sensors in the iterated-corrector probability hypothesis density (PHD) filter," *Proc. SPIE*, vol. 8050, May 2011, Art. no. 80500M.
- [32] R. Mahler, "Approximate multisensor CPHD and PHD filters," in *Proc. 13th Conf. Inf. Fusion (FUSION)*, Jul. 2010, pp. 1–8.
- [33] L. Liu, H. Ji, and Z. Fan, "A cardinality modified product multi-sensor PHD," *Inf. Fusion*, vol. 31, pp. 87–99, Sep. 2016.
- [34] D. Schuhmacher, B.-T. Vo, and B.-N. Vo, "A consistent metric for performance evaluation of multi-object filters," *IEEE Trans. Signal Process.*, vol. 56, no. 8, pp. 3447–3457, Aug. 2008.
- [35] T. Li, V. Elvira, H. Fan, and J. M. Corchado, "Local-diffusion-based distributed SMC-PHD filtering using sensors with limited sensing range," *IEEE Sensors J.*, vol. 19, no. 4, pp. 1580–1589, Feb. 2018.
- [36] G. Battistelli, L. Chisci, C. Fantacci, A. Farina, and A. Graziano, "Consensus CPHD filter for distributed multitarget tracking," *IEEE J. Sel. Topics Signal Process.*, vol. 7, no. 3, pp. 508–520, Jun. 2013.



LONG LIU was born in Xi'an, China, in 1988. He received the B.Eng. degree in electronic science and technology and the M.S. and Ph.D. degrees in pattern recognition and intelligent systems from Xidian University, China, in 2010, 2013, and 2016, respectively.

He is currently a Lecturer with the School of Electronic Engineering, Xidian University. His research interests include machine learning, signal processing, multi-target tracking, and data fusion.



WENBO ZHANG was born in Xi'an, China, in 1985. He received the B.Eng. degree in electronic science and technology and the M.S. and Ph.D. degrees in pattern recognition and intelligent systems from Xidian University, China, in 2005, 2009, and 2014, respectively.

He is currently a Lecturer with the School of Electronic Engineering, Xidian University. His research interests include machine learning, image processing, and target recognition.



HONGBING JI (M'96–SM'07) received the B.S. degree in radar engineering from the Northern West Telecommunications Engineering College (now Xidian University), Xi'an, China, in 1983, and the M.S. degree in circuit, signals and systems and the Ph.D. degree in signal and information processing from Xidian University, in 1989 and 1999, respectively, where he has been with the School of Electronic Engineering, since 1989.

He is currently a Professor and an Advisor for Ph.D. students. His research interests include radar signal processing, automatic targets recognition, multi-sensor information fusion, and target tracking.



GUISHENG LIAO and received the B.S. degree in mathematics from Guangxi University, Nanning, China, in 1983, and the M.S. degree in circuit, signals and systems and the Ph.D. degree in signal and information processing from Xidian University, in 1990 and 1992, respectively, where he has been with the School of Electronic Engineering, since 1990.

He is currently a Professor and an Advisor for Ph.D. students. His research interests include signal detection and estimation, adaptive signal processing, and array signal processing.

...